Islamic University of Gaza
Higher Education Deanery
Faculty of Science
Physics Department

Thermal – Stress Effects On TE Nonlinear Waveguide Sensors

By

Ghalea M. Abu Tair

Supervised By

Prof. Dr. M. M. Shabat

Submitted to the Faculty of Science as a Partial Fulfillment of the Master of Science (M.Sc.) in Physics

1428 - 2007

قال تعالى:

﴿ وَقُل رَّبِّ زِدْنِي عِلْمًا ﴾

صدق الله العظيم

To my ...

Parents, Husband and Sons.

ACKNOWLEDGEMENT

It gives me pleasure to thank my supervisor Prof. Dr. Mohammed M. Shabat for his valuable guidance and helpful supervision throughout this work. I would also like to thank Dr. Hala J. El-Khozondar, Dr. Samir Yassin and Dr. Ali El Assthal for their rich comments.

I would like to thank Dr. Mazen M. AL-Abadla for his fruitful discussion, important suggestions, and continuous support. Also, I would like to thank Mrs. Khetam U. El Wasife for her help and encouragement.

My thanks also go to the members of Physics department, at the Islamic University of Gaza.

I'm deeply thankful to my family for their encouragement and special thank goes to my husband for his cooperation, and patience that kept me productive during this work.

ملخص البحث

تناول البحث الوصلة أو القناة المستخدمة في الاتصالات لنقل المعلومـات مـن مكان إلى آخر؛ بواسطة انتشار الموجات الكهرومغناطيسية خلال أكثر من وسط، كـان الهدف هو اختيار المواد المناسبة ذات الجودة والكفاءة العالية.

فرض البحث ثلاثة أوساط على شكل شرائح بنفاذية مختلفة؛ وهي عبـارة عـن وسط خطي محاط من أعلاه ومن أسفله بوسطين غير خطيين، ويخضع الوسط الخطي لتأثير الحرارة والضغط الساكن عليه كلا على حدة؛ وقد اعتمد البحث علـى دراسـات نظرية سابقة في هذا المجال مثل دراسة العالم "هوانغ" على ثلاثة أوساط جميعها خطية.

وباستخدام معادلات "ماكسويل"؛ تم اشتقاق مركبات المجال الكهربي لكل وسـط ومعادلة التشتت للنظام المفروض والتعرف على حساسية درجة الحـرارة؛ التـي مـن خلالها تمكنت الباحثة من رسم أكثر من منحنى بواسطة برنامج رياضي خاص.

اتضح من النتائج النهائية للبحث انه يمكن استخدام الأوساط المفروضة في كثير من الأجهزة الفيزيائية في الصناعة، وكان من أبرز الدوافع الأخرى لهذا البحث أنها من الموضوعات الهامة في عصرنا الحالي.

ومن الممكن أن يكون هذا البحث مقدمة لأبحاث أخرى فـي مجـال الألياف الضوئية؛ باستخدام تأثير الحرارة والضغط على أوساط متعددة (أكثر من ثلاثة).

ABSTRACT

In recent years, waveguide sensors in dielectric films have received more attention. Many theoretical studies concerning analysis of dispersion equations were introduced for many planar waveguide structures for both linear and nonlinear media.

In this work, the TE electromagnetic waves in a three- layer waveguide sensors is studied. The waveguide structure is linear dielectric film bounded by two nonlinear cladding and substrate.

The dispersion relation of the electromagnetic field in the proposed structure has been derived. Numerical calculations are carried out. Consequently; effect of stress and thermal- stress on the core of the structure has been studied. Temperature sensitivity is also measured. These results were simulated and presented in graphical form using software program called Maple V.

PREFACE

Optical waveguides exhibit a number of interesting properties that have been investigated over the last years because of their application in all optical signal processing [6-10]. A great attention is nowadays paid to optical waveguide sensors because they offer many advantages such as: small size and capability of performing multi-functional sensor on one chip [16-20]. Since then, varieties of sensors have been developed and theoretical analysis of novel devices has been proposed. Most of the studies has focused on such waveguide sensors, that have three layers in which all layers are linear or at least one is nonlinear [21-24]. Huang studied the effect of thermal-stress on three layers linear waveguide sensors. He introduced temperature sensitivity and studied the effect of various kinds of stresses on performance [8, 26]. El-Khozondar, et. al.(2006) have investigated the thermal, and stress effects on a three layer nonlinear waveguide sensors where one layer is a nonlinear medium [35].

In the present work we study the s-polarized nonlinear surface electromagnetic waves supported by three layers structure consisting of linear dielectric film, bounded by nonlinear cover and substrate. The temperature sensitivity of optical waveguide structure could be controlled by thermal- stress and stress too. The aim of this study is to examine the influence of nonlinearity and thermal stress on sensitivity.

The first chapter contains definitions and basis for analytical investigation of the present work. In chapter two, we review the general solution for linear waveguide sensors with stress and thermal- stress

effect. Chapter three gives a full description of optically nonlinear waves in thin film without thermal- stress.

In chapter four, we derive a new exact analytical dispersion equation of a nonlinear TE waves propagating in the proposed waveguide structure and the nonlinear sensitivity is calculated. Finally, the results are plotted, discussed, and analyzed in chapter five.

CONTENTS

List of figures

CHAPTER 1

General Survey

1.1 Introduction

This introductory chapter deals with the fundamental ideas needed to carry out this work. The concept of three – layered optical planar waveguides are considered. Solutions of Maxwell's equations in linear and nonlinear media are discussed. The fundamentals of optical sensing processes are also studied.

1.2 Planer waveguides

Optical waveguides are basic components in many optical systems. It consists of layer of high refractive index material called the core surrounded with other lower refractive index called the cladding[1].

We can define the effective refractive index (N) of the guided mode traveling along the guiding film as the ratio of speed of light in vacuum to the effective speed along the guide. (N) is different for the different modes and *does* depend on the refractive index, thickness of waveguide film and the surroundings.

$$N = \frac{k}{k_o} \qquad (1.1)$$

(k_o , k) are the wave numbers of free space and medium respectively [2,6]. In general, sensing process consists of measuring the change of the effective index of a propagating mode according to either changes of refractive index in the waveguide cover or changes in thickness of the core [7].

The type of waveguides currently used in biochemical and medical sensing is planar optical waveguide structure. We can consider planar waveguide slab consist of three – layer settled on the x-y plane and x-direction will be considered the propagation direction of guided modes, the guide is therefore a film of dielectric non – magnetic material [8].

The electric field **E** and the magnetic field **H** for the system in general can be written as [9]:

$$\boldsymbol{E} = [\, E_x \boldsymbol{i} + E_y \boldsymbol{j} + E_z \boldsymbol{k} \,] \,.\, exp[i\,(kx - \omega t)] \tag{1.2.a}$$

$$\boldsymbol{H} = [\, H_x \boldsymbol{i} + H_y \boldsymbol{j} + H_z \boldsymbol{k} \,] \,.\, exp[i\,(kx - \omega t)] \tag{1.2.b}$$

where ω is the angular frequency and t is time.

1.3 Maxwell's equation for optical planar waveguide

In dielectric media, the electric and magnetic fields must, of course, satisfy Maxwell's equations, in the planar waveguide as:

$$(i)\ \nabla . \boldsymbol{E} = 0 \tag{1.3.a}$$

$$(ii)\ \nabla . \boldsymbol{H} = 0 \tag{1.3.b}$$

$$(iii)\ \nabla \times \boldsymbol{E} = -\,\mu \frac{\partial \boldsymbol{H}}{\partial t} \tag{1.3.c}$$

$$(iv)\ \nabla \times \boldsymbol{H} = \varepsilon \frac{\partial \boldsymbol{E}}{\partial t} \tag{1.3.d}$$

Where μ, ε are permeability and permittivity respectively of the media, for free space $\mu = \mu_0$ and $\varepsilon = \varepsilon_0$.

Using eq.(1.2), we find the following relations:

$$E_x = -\frac{i}{k}\frac{\partial E_z}{\partial z} = -\frac{i}{\omega \varepsilon_o \varepsilon}\frac{\partial H_y}{\partial z} \tag{1.4.a}$$

$$H_x = \frac{i}{k}\frac{\partial H_z}{\partial z} = \frac{i}{\omega\ \mu_o}\frac{\partial E_y}{\partial z} \quad (1.4.b)$$

$$\frac{\partial E_x}{\partial z} = i\,k\,E_z + i\,\mu_o\,\omega\,H_y \quad (1.4.c)$$

$$\frac{\partial H_x}{\partial z} = i\,k\,H_z - i\,\omega\,\varepsilon_o\,\varepsilon_i\,E_y \quad (1.4.d)$$

$$E_y = \frac{\omega\mu_o}{k}H_z \quad (1.4.e)$$

$$H_y = -\frac{\omega\varepsilon_o\varepsilon_i}{k}E_z \quad (1.4.f)$$

Where ε_o is the permittivity of the free space, μ_o is the permeability of free space and ε_i is the relative permittivity in the medium [3].

If eq (1.4.c) and eq (1.4.d) are differentiated with respect to z, we obtained:

$$\frac{\partial^2 E_x}{\partial z^2} + \left(\frac{\omega^2}{c^2}\varepsilon - k^2\right)E_x = 0 \quad (1.5.a)$$

$$\frac{\partial^2 H_x}{\partial z^2} + \left(\frac{\omega^2}{c^2}\varepsilon - k^2\right)H_x = 0 \quad (1.5.b)$$

where $c = \frac{1}{\sqrt{\varepsilon_o\mu_o}}$ is the speed of light in vacuum [8] .

1.4 Types of transverse field

Equations (1.5.a) and (1.5.b) show that E_x and H_x are uncoupled, this uncoupling is necessary, and sufficient to obtain the condition for the existence of TE and TM modes [9].

(i) *- Transverse electric field (TE):*

In the transverse electric field [6] (s-polarized) the electric field **E** is perpendicular to the plane of incidence, and the magnetic field **H** is parallel to it, that is:

$$\mathbf{E}= (0, E_y , 0) \, . \, exp[i \, (kx - \omega t)] \qquad (1.6.a)$$

$$\mathbf{H}= (H_x, 0 , H_z) \, . \, exp[i \, (kx - \omega t)] \qquad (1.6.b)$$

(ii) *- Transverse magnetic field (TM):*

In the transverse magnetic field (p-polarized) the magnetic field H is normal to the plane of incidence, and the electric field E is parallel to it that is:

$$\mathbf{E}= (E_x, 0 , E_z) \, . \, exp[i \, (kx - \omega t)] \qquad (1.7.a)$$

$$\mathbf{H}= (0, H_y , 0) \, . \, exp[i \, (kx - \omega t)] \qquad (1.7.b)$$

There is a finite number of discrete modes, and the field distributions associated with the few TE_m waves. Figure 1.1 exhibits the field distribution for three TE wave modes. It can be seen that fields executes oscillatory behavior in the film, and decay exponentially with distance into the cladding and substrate [10].

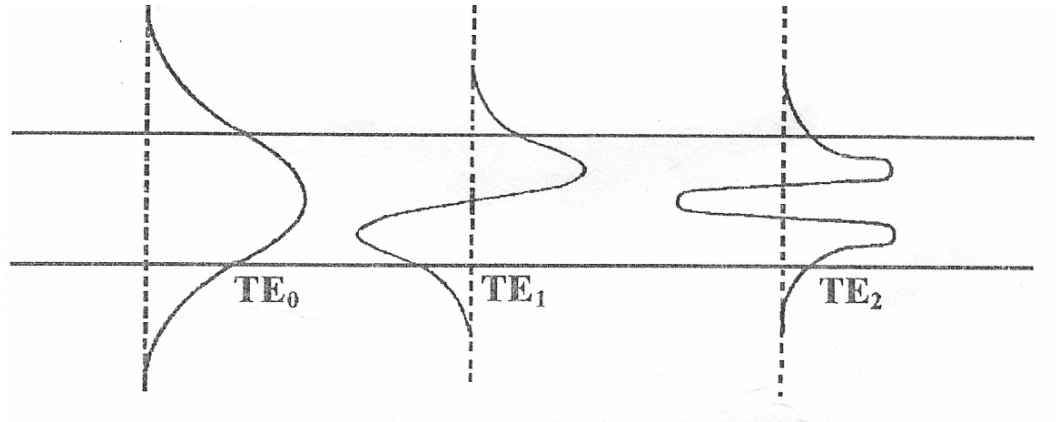

Figure.1.1:Typical electric field distributions for TE_m modes

1.5 TE waves Linear and nonlinear

TE waves can introduced by two kind of waves in which the dielectric constants dependent on field strength (nonlinear) or does not depend on field strength (linear).

1.5.a Linear TE waves

Suppose the fields are TE waves, which propagates along the x-axis. The field components of these waves are shown in eq. (1.6). If this wave propagates in a medium that has a linear dielectric constant (ε), then the field equation for this medium is given as :

$$\frac{\partial^2 Ey}{\partial z^2} - k_o^2 (N^2 - \varepsilon) Ey = 0 \qquad (1.8)$$

The differential eq. (1.8) can have two kinds of solutions:

1- surface wave ($N^2 > \varepsilon$), $N^2 - \varepsilon$ is positive quantity, then the solution in the medium is given by :

$$E_y = A\cosh(k_o qz) + B\sinh(k_o qz), \qquad (1.9)$$

$$q = \sqrt{N^2 - \varepsilon}$$

2- propagating wave($N^2 < \varepsilon$), $N^2 - \varepsilon$ is negative quantity, then the oscillatory solution in the medium is given by:

$$E_y = C\cos(k_o qz) + D\sin(k_o qz) \qquad (1.10)$$

Where A, B, C and D are constants which can computed by using boundaries conditions.

1.5.b Nonlinear TE waves

In Nonlinear medium the dielectric constant depends on field strength and is given by [9, 27]:

$$\varepsilon^{Nl} = \varepsilon^{L} + \alpha \ |E|^2 \tag{1.11}$$

Where α_t is nonlinearity coefficient, ε^{NL} is the dielectric constant for nonlinear medium and ε^{L} is the dielectric constant for linear medium. Substituting in eq. (1.5.a) leads to the differential equation[9, 15]:

$$\frac{\partial^2 E_y}{\partial z^2} - k_o^2 (N^2 - \varepsilon_r^{NL}) E_y + \alpha k_o^2 E_y^3 = 0 \tag{1.12}$$

According to α values this differential equation has two solutions:

$$E_y = \sqrt{\frac{2}{\alpha}} \frac{q}{\cosh\left(k_o q \ (z - z_c)\right)} \qquad \text{for} \quad \alpha > 0 \tag{1.13.a}$$

$$E_y = \sqrt{\frac{2}{\alpha}} \frac{q}{\sinh\left(k_o q \ (z - z_c)\right)} \qquad \text{for} \quad \alpha < 0 \tag{1.13.b}$$

$z_c$is a constant related to the power of the waveguide, more specifically, the field peaks at $z = z_c$.

In the case where α is positive ($\alpha > 0$), the medium is said to be self – focusing, whereas for the caseα is negative ($\alpha < 0$), the medium is said to be self – defocusing [14- 16].

1.6 Power flow in guided waves

The guided wave power per unit length (**P**) in units of (watt/m) or (m watt/m m) along the y-axis is obtained in the usual way by integrating the Poynting vector over the depth dimension [2, 10, 27] as:

$$\mathbf{S} = \mathbf{E} \times \mathbf{H} \tag{1.14}$$

Where **S** (watts/m^2) is the amount of flow energy on unit surface of any volume (V). The integration of this quantity over the closed surface gives the power flow associated with the wave.

Invariably a time-harmonic field[$exp(-i\omega t)$]is used so that instead of **S**, we should use the time average over one period. This is given mathematically as:

$$\begin{aligned} <\mathbf{S}> &= <\mathrm{Re}(\mathbf{E}) \times \mathrm{Re}(\mathbf{H})> \\ &= <1/2(\mathbf{E}+\mathbf{E}^*) \times 1/2(\mathbf{H}+\mathbf{H}^*)> \end{aligned} \tag{1.15}$$

Notice that $<\mathbf{E} \times \mathbf{H}> = <\mathbf{E}^* \times \mathbf{H}^*> = 0$ over one period. This gives:

$$<\mathbf{S}> = 1/2\ \mathrm{Re}(\mathbf{E} \times \mathbf{H}^*) = 1/2\ \mathrm{Re}(\mathbf{E}^* \times \mathbf{H}) \tag{1.16}$$

Where * denotes the complex conjugate (imaginary part) and Re means that the real part is taken.

Finally , $P = \frac{1}{2}\int(\mathbf{E} \times \mathbf{H}^*)\ dz$

In the case of **TE** waves propagates down the x-axis < **S** > is follow as :

$$<\mathbf{S}> = \frac{1}{2}\mathrm{Re}\begin{vmatrix} \mathbf{i} & \mathbf{j} & \mathbf{k} \\ 0 & E_y & 0 \\ \dfrac{-i}{\omega\mu_o}\dfrac{\partial E_y}{\partial z} & 0 & \dfrac{k}{\omega\mu_o}E_y \end{vmatrix} = \frac{1}{2}\frac{k}{\omega\,\mu_o}E_y^2\ \mathbf{i} \tag{1.17}$$

Where $\mathbf{H}_x = \dfrac{i}{\omega\ \mu_o}\dfrac{\partial E_y}{\partial z}$, $\mathbf{H}_z = \dfrac{k}{\omega\ \mu_o}E_y$

This formula can be used for both linear and nonlinear TE.

For **TM** waves < **S** > is given below:

$$< \mathbf{S} > = \frac{1}{2}\mathrm{Re}\begin{vmatrix} \mathbf{i} & \mathbf{j} & \mathbf{k} \\ \dfrac{-i}{\omega \varepsilon_o \varepsilon}\dfrac{\partial H_y}{\partial z} & 0 & -\dfrac{k}{\omega \varepsilon_o \varepsilon}E_y \\ 0 & H_y & 0 \end{vmatrix} = \frac{1}{2}\frac{\omega \mu_o \varepsilon}{k}E_z^2 \mathbf{i} \qquad (1.18)$$

This formula is also applied for nonlinear TM waves [10- 16].

1.7 Optical sensors

Optical Sensors are used for optical communication and made of transparent dielectrics whose function is to guide visible and infrared light over long distance. Optical sensors are very important components for the measurement of biological, physical and chemical quantity as detecting the concentration of certain chemical blood. Sensors based on the design and fabrication of a physical transducer that can transform the chemical or biological reaction into a measurable signal. Sensing is performed by the evanescent penetration of the field in the cover medium, and is proportional to the fraction of evanescent power flow in the cover. Due to their importance in bio-sensing application, various optical sensors based on evanescent wave concept have been developed [17].

Optical Sensing is mainly used in concentration monitoring, measuring traces of chemicals and studying all physical and chemical properties that change in accordance with changes in refractive index which depends on film thickness and refractive indices of both film and surroundings [18, 19].

Optical sensing is very important in both research and industry because of their miniature, high sensitivity, small size, immunity to electromagnetic interference and low price [20].

In recent years several planar optical waveguide sensors have been suggested for biological applications. The detection of pathogenic bacteria have received renewed interest, especially within the fields of food safety, medical diagnostics, and biological warfare. Typically, optical waveguide sensors are used for measuring the refractive index of liquids or various aqueous solutions of biological substances, such as mammalian cells, bacterial cells, and proteins .

There are another application for optical waveguide sensors that can be used for detecting and measuring the thickness of layers such as metals, metal compounds, organic, bio-organic, enzymes, antibodies and microbes. They are also used in radiation dosimeters and protective masks or clothing when they can readily identify and give scanning data about any change in exposure or lack in protection [12, 13].

1.8 Schemes of sensing and the sensitivity

Sensing is performed by the evanescent tail of the modal field in the cover medium. In general, sensing process consists of measuring the change of the effective index of a propagating mode according to either changes of refractive index in the waveguide cover or changes in thickness of the core [7].

The sensitivity of the measurement of the physical or chemical quantity present in the cover depends on the strength and the distribution of the evanescent field in the cover, Therefore there is the temperature sensitivity which defined as the rate of effective refractive index respect to temperature.

There are two types of sensing as shown in figure 1.2, where n_c, n_g, n_s, and n_f are the refractive indices for cover, core, substrate, and film respectively:

a) Homogeneous sensing

In which the properties of waveguide cover are distributed homogenously, and the sensitivity for this sensing is defined as the rate of change of the model effective refractive index under an index change of the cover as shown in figure (1.2.a).

b) Surface sensing

In which an ultra- thin film rests on guiding film. In this configuration, changes in optical properties are due to adsorption of some molecules that construct an ultra thin- film. The sensitivity of surface sensing structure is defined as the rate of change of the model effective index with respect to changes in ad- layer width as shown in figure (1.2.b) [17] .

1.9 Aim of work

We will study the TE- nonlinear surface electromagnetic waves supported by a three- layer structure, consisting of a linear dielectric film, surrounded by nonlinear cladding and nonlinear substrate too. Dispersion relationship and numerical results for this structure will be obtain then present in graphical form and discussed. This study of three- layer structure that considered in the present work can support symmetric modes, which investigated by *Huang* [8].

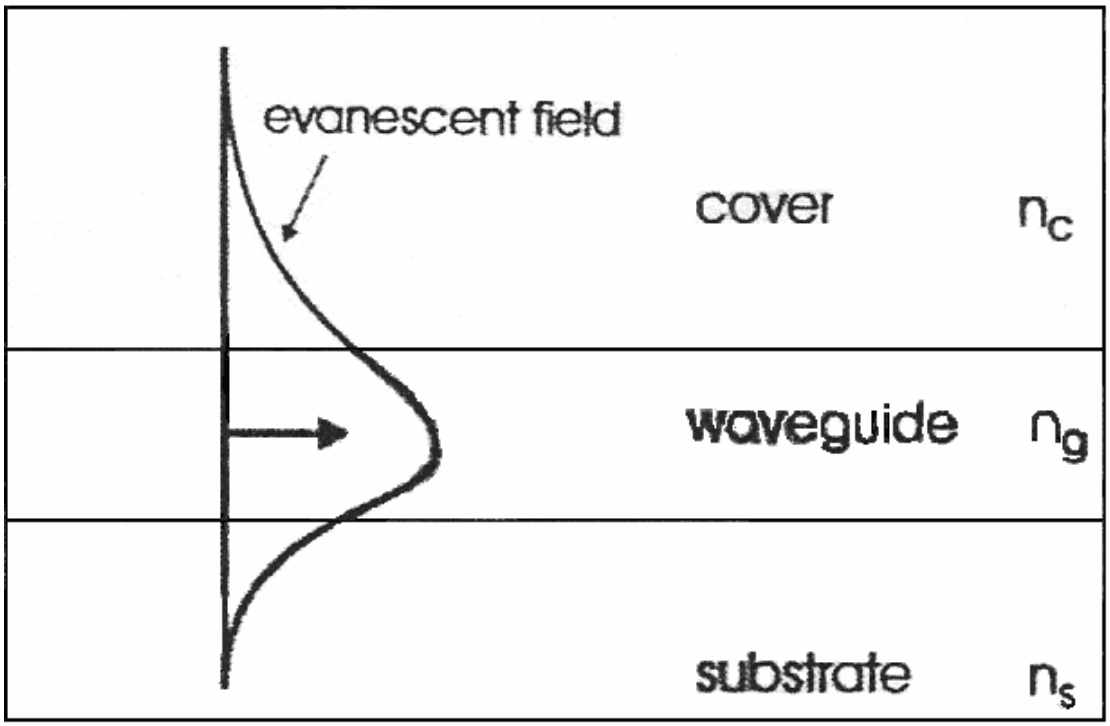

(a)

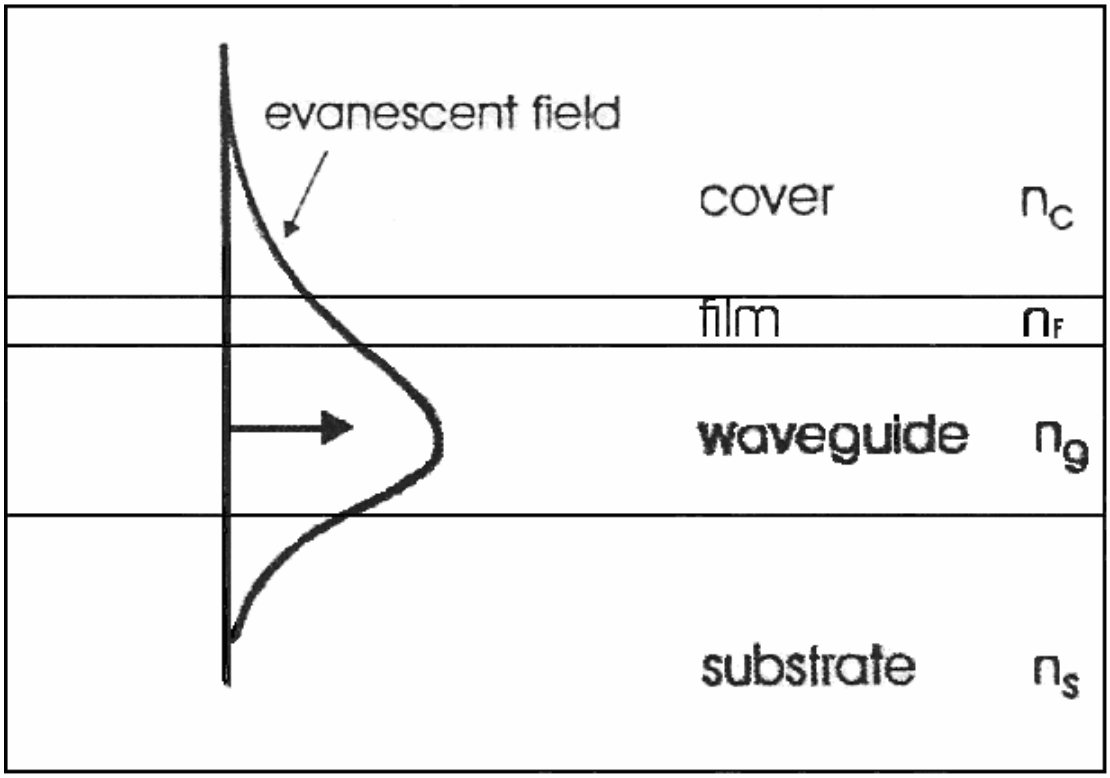

(b)

Figure .1.2: Schematic representation of (a) Homogeneous sensor and (b) surface sensor.

CHAPTER 2

Effect of Thermal- Stress and Stress on Linear Optical Waveguide Sensors

The stress effects on the refractive index of a dielectric and on the performance of optical waveguide sensors are widely studied [8].
This chapter gives a theoretical analysis and a fundamental mathematical concepts of temperature-dependent linear waveguide sensors. The dispersion relation and the temperature sensitivity for linear media have been derived. Stress and thermal - stress effect on optical waveguide sensors are discussed.

2.1 Thermal–Stress effects on optical properties of dielectric materials

In anisotropic and inhomogeneous medium The dielectric tensor of, ε, is given by [8, 29]:

$$\varepsilon = \begin{bmatrix} n_{xx}^{\,2} & n_{xy}^{\,2} & n_{xz}^{\,2} \\ n_{yx}^{\,2} & n_{yy}^{\,2} & n_{yz}^{\,2} \\ n_{zx}^{\,2} & n_{zy}^{\,2} & n_{zz}^{\,2} \end{bmatrix} \quad , \tag{2.1}$$

where the refractive indices n_{xx} , n_{yy}, n_{zz}, n_{xy}, and n_{yz} are Functions of temperature, stress, and wavelength. The relation between the refractive index and temperature (thermo – optic relation) is

$$\frac{\partial n}{\partial T} = Bn \quad , \tag{2.2}$$

where T is temperature and B is the thermo-optic coefficient, which is usually a function of the refractive index, wavelength and temperature. [26].

Thermal stresses vary with temperature. Combining thermo-optic and elasto-optic relations gives the refractive index change with temperature in the form:

$$\Delta\begin{pmatrix} n_{xx} \\ n_{yy} \\ n_{zz} \\ n_{yz} \\ n_{xz} \\ n_{xy} \end{pmatrix} = B\Delta T\begin{pmatrix} n_{xx} \\ n_{yy} \\ n_{zz} \\ n_{yz} \\ n_{xz} \\ n_{xy} \end{pmatrix} - \begin{pmatrix} c_2 & c_2 & c_2 & 0 & 0 & 0 \\ c_2 & c_1 & c_2 & 0 & 0 & 0 \\ c_2 & c_2 & c_1 & 0 & 0 & 0 \\ 0 & 0 & 0 & c_3 & 0 & 0 \\ 0 & 0 & 0 & 0 & c_3 & 0 \\ 0 & 0 & 0 & 0 & 0 & c_3 \end{pmatrix}\begin{pmatrix} \Delta\sigma_{xx} \\ \Delta\sigma_{yy} \\ \Delta\sigma_{zz} \\ \Delta\sigma_{yz} \\ \Delta\sigma_{xz} \\ \Delta\sigma_{xy} \end{pmatrix} \tag{2.3}$$

where c_1, c_2, and c_3, are stress-optic constant, σ_{xx}, , σ_{yy}, σ_{zz}, σ_{yz}, σ_{xz}, σ_{xy} are the stress components.

The change of refractive index, Δn, is affected by temperature change, ΔT, and stress change, $\Delta\sigma$, change is considered linear with temperature, upon changing temperature from T_o to T. Stresses in the waveguide at temperature T are written as:

$$\begin{bmatrix} \sigma_{xx} & \sigma_{xy} & \sigma_{xz} \\ \sigma_{xy} & \sigma_{yy} & \sigma_{yz} \\ \sigma_{xz} & \sigma_{yz} & \sigma_{zz} \end{bmatrix} \tag{2.4}$$

the refractive indices at temperature T can be obtained from eq. (2.3) as

$$\begin{pmatrix} n_{xx} \\ n_{yy} \\ n_{zz} \\ n_{yz} \\ n_{xz} \\ n_{xy} \end{pmatrix} = [1 + B(T - T_o)] \begin{pmatrix} n_0 \\ n_0 \\ n_0 \\ 0 \\ 0 \\ 0 \end{pmatrix} - \begin{pmatrix} c_2 & c_2 & c_2 & 0 & 0 & 0 \\ c_2 & c_1 & c_2 & 0 & 0 & 0 \\ c_2 & c_2 & c_1 & 0 & 0 & 0 \\ 0 & 0 & 0 & c_3 & 0 & 0 \\ 0 & 0 & 0 & 0 & c_3 & 0 \\ 0 & 0 & 0 & 0 & 0 & c_3 \end{pmatrix} \begin{pmatrix} \sigma_{xx} \\ \sigma_{yy} \\ \sigma_{zz} \\ \sigma_{yz} \\ \sigma_{xz} \\ \sigma_{xy} \end{pmatrix} \qquad (2.5)$$

where n_o is the refractive index at temperature T_o and under the stress-free state [11, 26].

In practical situation, a waveguide is usually exposed to a very complicated form of stress, both in homogeneity and anisotropy exist. Therefore the stress state in the core can be expressed as:

$$\begin{aligned} \sigma_{xx} &= g_x E \Delta\alpha (T - T_0) + \sigma_{rx} \\ \sigma_{yy} &= g_y E \Delta\alpha (T - T_0) + \sigma_{ry} \\ \sigma_{zz} &= g_z E \Delta\alpha (T - T_0) + \sigma_{rz} \\ \sigma_{yz} &= \sigma_{xz} = \sigma_{xy} = 0 \end{aligned} \qquad (2.6)$$

where E is Young's modulus of the core which defined as a measure of the elasticity of a material which does not depend on the shape or size of the piece of material, $\Delta\alpha = \alpha_{cladding} - \alpha_{core}$ is the thermal- expansion coefficient mismatch between the cladding and core; σ_{rx}, σ_{ry} and σ_{rz} are residual stresses along x, y, and z directions, which are independent of temperature, g_x, g_y, and g_z are loading parameters, which are functions of Young's modulus ratio.

In the following analysis the stress in the core is assumed to be homogenous, and the thermal stress in the core is assumed to be only due to the thermal mismatch between the core and cladding, this will give:

$$g_x = 0$$

$$g_y = g_z = 1/(1-\nu) \tag{2.7}$$

where ν is Poisson's ratio.

Under the stress state given in eq. (2.6), the refractive-index profile of the core can be obtained from eq. (2.5) as:

$$n_{xx} = n_0 + Bn_0(T-T_0) - c_1(g_x E\Delta\alpha(T-T_0) + \sigma_{rx}) - c_2(g_y E\Delta\alpha(T-T_0) + \sigma_{ry}) - c_2(g_z E\Delta\alpha(T-T_0) + \sigma_{rz})$$

$$n_{xx} = n_0 + (T-T_0)(Bn_0 - c_1 g_x E\Delta\alpha - c_2 g_y E\Delta\alpha - c_2 g_z E\Delta\alpha) - c_1\sigma_{rx} - c_2\sigma_{ry} - c_2\sigma_{rz}$$

$$n_{xx} = n_0 + [Bn_0 - c_1 g_x E\Delta\alpha - c_2(g_y + g_z)E\Delta\alpha] \times (T-T_0) - c_1\sigma_{rx} - c_2(\sigma_{ry} + \sigma_{rz}) \tag{2.8.a}$$

$$n_{yy} = n_0 + Bn_0(T-T_0) - c_2(g_x E\Delta\alpha(T-T_0) + \sigma_{rx}) - c_1(g_y E\Delta\alpha(T-T_0) + \sigma_{ry}) - c_2(g_z E\Delta\alpha(T-T_0) + \sigma_{rz})$$

$$n_{yy} = n_0 + (T-T_0)(Bn_0 - c_2 g_x E\Delta\alpha - c_1 g_y E\Delta\alpha - c_2 g_z E\Delta\alpha) - c_2\sigma_{rx} - c_1\sigma_{ry} - c_2\sigma_{rz}$$

$$n_{yy} = n_0 + [Bn_0 - c_1 g_y E\Delta\alpha - c_2(g_x + g_z)E\Delta\alpha] \times (T-T_0) - c_1\sigma_{ry} - c_2(\sigma_{rx} + \sigma_{rz}) \tag{2.8.b}$$

$$n_{zz} = n_0 + Bn_0(T-T_0) - c_2(g_x E\Delta\alpha(T-T_0) + \sigma_{rx}) - c_2(g_y E\Delta\alpha(T-T_0) + \sigma_{ry}) - c_1(g_z E\Delta\alpha(T-T_0) + \sigma_{rz})$$

$$n_{zz} = n_0 + (T - T_0)(Bn_0 - c_2 g_x E\Delta\alpha - c_2 g_y E\Delta\alpha - c_1 g_z E\Delta\alpha) - c_2\sigma_{rx} - c_2\sigma_{ry} - c_1\sigma_{rz}$$

$$n_{zz} = n_0 + [Bn_0 - c_1 g_z E\Delta\alpha - c_2 (g_x + g_y) E\Delta\alpha] \times (T - T_0) - c_1\sigma_{rz} - c_2(\sigma_{rx} + \sigma_{ry}) \quad (2.8.c)$$

2.2 Dispersion equation of linear planer waveguide

Consider a symmetric, infinitely large planar waveguide sensor with very thick cladding regions as shown in figure 2.1. The light is confined in the core region with thickness t, propagates in the x-direction, and has no variation in the y- direction [21, 22]. The waveguide is assumed under the homogenous stress state, and the cladding does not have an elasto – optic effect.

In a TE configuration, the Maxwell's equation of the core is:

$$\frac{\partial^2 E_y}{\partial z^2} - k_o^2 (N^2 - \varepsilon_f) E_y = 0 \quad (2.9)$$

The equation for the cladding is:

$$\frac{\partial^2 E_y}{\partial z^2} - k_o^2 (N^2 - \varepsilon_c) E_y = 0 \quad (2.10)$$

The equation for the substrate is :

$$\frac{\partial^2 E_y}{\partial z^2} - k_o^2 (N^2 - \varepsilon_s) E_y = 0 \quad (2.11)$$

where $k = 2\pi/\lambda$, λ is the wavelength, ε_f is the dielectric constant of the core, N is the effective refractive index of the TE mode, and ε_c, ε_s is the dielectric constant for the cladding and substrate respectively.

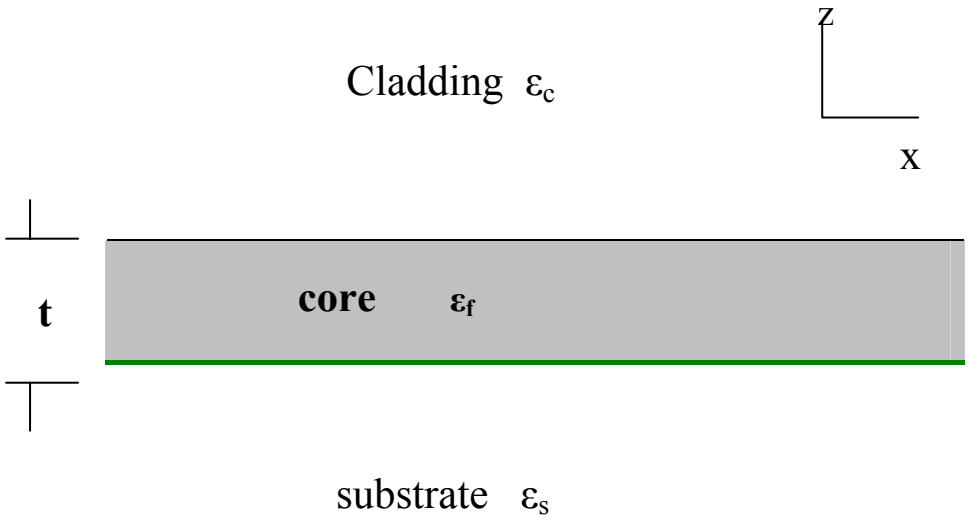

Fig.2.1: Schematic of a symmetric three –layer planar waveguide.

The general solution of Maxwell's equations, eq. (2.9), eq. (2.10) and eq. (2.11) respectively takes the general form as:

$$E_y = A\cosh(k_o qz) + B\sinh(k_o qz) \tag{2.12}$$

$$E_y = A_c \exp(-k_o qz) \tag{2.13}$$

$$E_y = A_s \exp(k_o qz) \tag{2.14}$$

where $p = \sqrt{N^2 - \varepsilon_f}$ and $q = \sqrt{(N^2 - \varepsilon_i)}$.

where A, B, A_c, A_s are constants can be determined from the boundary condition.

Continuity of both E_y, $\frac{\partial E_y}{\partial z}$ at the boundaries (z = 0 and z = t) will give the dispersion equation, eq. (2.15) [11, 24]:

$$k_o tp - 2\arctan(\frac{q}{p}) - m\pi = 0 \tag{2.15}$$

where m = 0,1,2,… .

For even values of m eq. (2.15) reduces to

$$p \tan(\frac{k_o tp}{2}) = q \tag{2.16.a}$$

For odd values of m, eq. (2.15) will be

$$q \tan(k_o tp/2) = -p \tag{2.16.b}$$

2.3 Stress effects on the performance of planer waveguides

Stresses can cause anisotropic and inhomogeneous distribution of the refractive index. The relation between refractive indices and the stress is found to be [4, 8]:

$$\begin{pmatrix} n_{xx} \\ n_{yy} \\ n_{zz} \\ n_{yz} \\ n_{xz} \\ n_{xy} \end{pmatrix} = \begin{pmatrix} n_0 \\ n_0 \\ n_0 \\ 0 \\ 0 \\ 0 \end{pmatrix} - \begin{pmatrix} c_2 & c_2 & c_2 & 0 & 0 & 0 \\ c_2 & c_1 & c_2 & 0 & 0 & 0 \\ c_2 & c_2 & c_1 & 0 & 0 & 0 \\ 0 & 0 & 0 & c_3 & 0 & 0 \\ 0 & 0 & 0 & 0 & c_3 & 0 \\ 0 & 0 & 0 & 0 & 0 & c_3 \end{pmatrix} \begin{pmatrix} \sigma_{xx} \\ \sigma_{yy} \\ \sigma_{zz} \\ \sigma_{yz} \\ \sigma_{xz} \\ \sigma_{xy} \end{pmatrix} \qquad (2.17)$$

Where $c_1 = n_0^3 (p_{11} - 2\nu p_{12}) / (2E)$, $c_2 = n_0^3 (p_{11} + p_{12}) / (2E)$ and $c_3 = n_0^3 (p_{44}) / (2G)$ are stress – optic constant. E, G and ν are Young's modulus, shear modulus and Poisson's ratio, respectively. For isotropic crystals, $p_{44} = (p_{11} - p_{12}) / 2$ and $G = E / 2(1 + \nu)$. In eq.(2.17), it is assumed that the refractive index of media is homogeneous and is defined in terms of the principal dielectric axes of the free stress state. Table (1) lists the photo-elastic constants of some material. Stress – optic constants, are calculated from strain – optic constants, *p*, listed in the book by Xu and Stroud (1992) [8].

The stresses in microstructures are usually on the order of 10^8 Pa, and the values in Table (1) are on the order of 10^{-11} Pa^{-1}, so the refractive index change caused by stress is normally between ± 0.01. Because the stresses are usually non- uniformly distributed (inhomogeneous) and have different values in different direction (anisotropic) in the waveguide, the refractive indices are also inhomogeneous and anisotropic.

To study the stress magnitude effect, referring to figure 2.1 we assumed the core is to be under hydrostatic stress state, i.e., $\sigma_{xx} = \sigma_{yy} = \sigma_{zz} = \sigma$ and $\sigma_{xy} = 0$, the value of the refractive index in the core changes due to the stress, i.e., $n_{xx} = n_{yy} = n_{zz} = n = n_0 - (c_1 + 2c_2)\,\sigma$. The mode equation of the core is simplified to

$$\frac{\partial^2 E_y}{\partial z^2} - k_o^2 (N^2 - \varepsilon_f) E_y = 0 \qquad (2.18)$$

Considering zero fields at large z, the above equation can be solved as for N_2 - ε_f positive quantity then the general solution of eq. (2.18) is given by [25]:

$$E_y = A\cosh(k_o q z) + B\sinh(k_o q z) \qquad (2.19)$$

At the interface between core and the two cladding the continuity of both E_y, $\frac{\partial E_y}{\partial z}$ at the interfaces (z = 0 and z = t) will give the values of the constants and the effective refractive index (N).

Table 1

The photo –elastic constants of some materials

Material	$\lambda_0(\mu m)$	n_0	P_{11}	P_{12}	P_{44}	$C_1(10^{-12}/pa)$	$C_2(10^{-12}/pa)$	$C_3(10^{-12}/pa)$
Ge	2.0-2.2	4	-0.063	-0.0535	-0.074	-10.56	-6.78	-35.29
	10.6		0.27	0.235	0.125	44.27	30.37	59.61
Si	1.15	3.42	-0.101	0.0094		-11.35	3.65	
	3.39		-0.094	0.017	-0.051	-11.04	4.04	-12.82
GaAs	1.15	3.43	-0.165	-0.140	-0.072	-18.39	-10.63	-24.46
Fused silica	0.633	1.46	0.121	0.270		0.65	4.50	-3.85
GaP	0.633	3.32	-0.151	-0.082	-0.074	-17.91	-1.87	-19.21
$LiNbO_3$	0.633	2.29	-0.026	0.090	0.146	-2.10	2.55	-14.63
LiTaO3	0.633	2.18	-0.084	0.081	0.028	-2.57	1.91	1.53
$Al_2 O_3$	0.633	1.76	-0.23	-0.03	-0.10	-1.61	0.202	-1.90
$PbMoO_4$	0.633	2.39	0.24	0.24	0.067	6.63	6.63	17.04

A computer program was developed to plot the relation between effective refractive index (N) and a thickness of the core(t) for m = 0, 1, 2 as shown in figure 2.2, where the value of the stress can take two values ($c_1\sigma = -0.01$) and ($c_1\sigma = 0.01$). In the figure, c_2/c_1 is considered 0.1, $\lambda = 0.83\mu m$, $n_o = 3.5$, $n_1 = 3$, and (t) can take the value from 0 to 1.5μm. This figure shows that the order– m = 0 has the largest values in both negative and positive stresses. It is clear that the highest values is achieved with negative stresses for m = 0.

Figure 2.3 shows the effective indices as a function of normalized stress for a 1 μm core thickness waveguide.
However, the effective indexes vary with stress, and the cutoff thickness, which is defined as the core thickness at which the field is no longer guided by the core (N = n_c in this case), shifts when the stress value is high. In figure 2.3, when t = 1 μm, the second mode (m = 2) appears (or disappears) when stress changes. This means that stress can cause multimode. The field distributions of the fundamental modes (m = 0) are shown in figure 2.4. The model field is normalized by the time-averaged power flow, *P*, which is given by Poynting vector, 1/2Re(**E**×**H***).

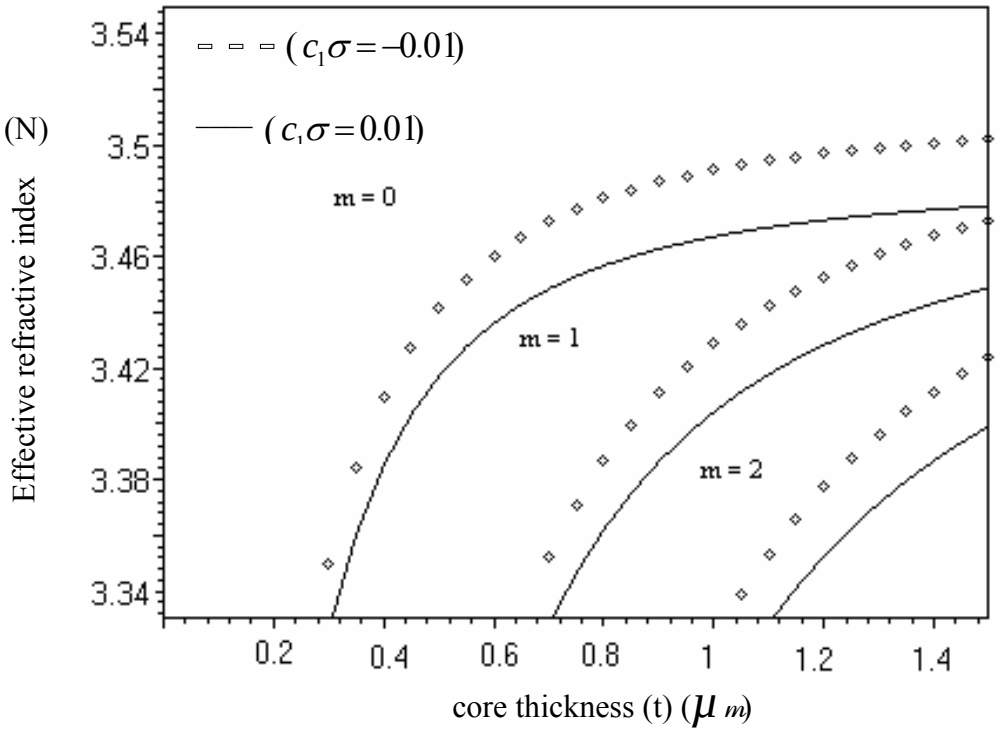

Fig.2.2: Effective refractive index (N) as a function of core thickness (t) for a symmetric planar optical waveguide under different hydrostatic stresses.

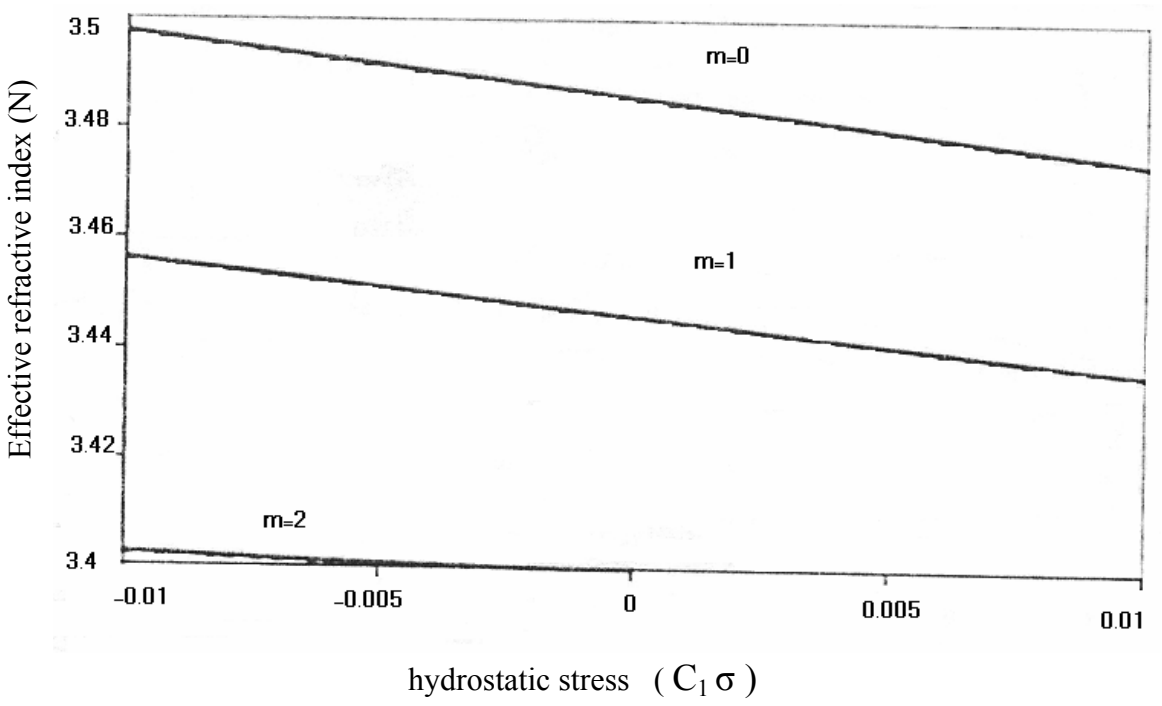

Fig.2.3: Effective refractive index (N) as a function of normalized hydrostatic stress for a symmetric planar optical waveguide with t = 1 μm .

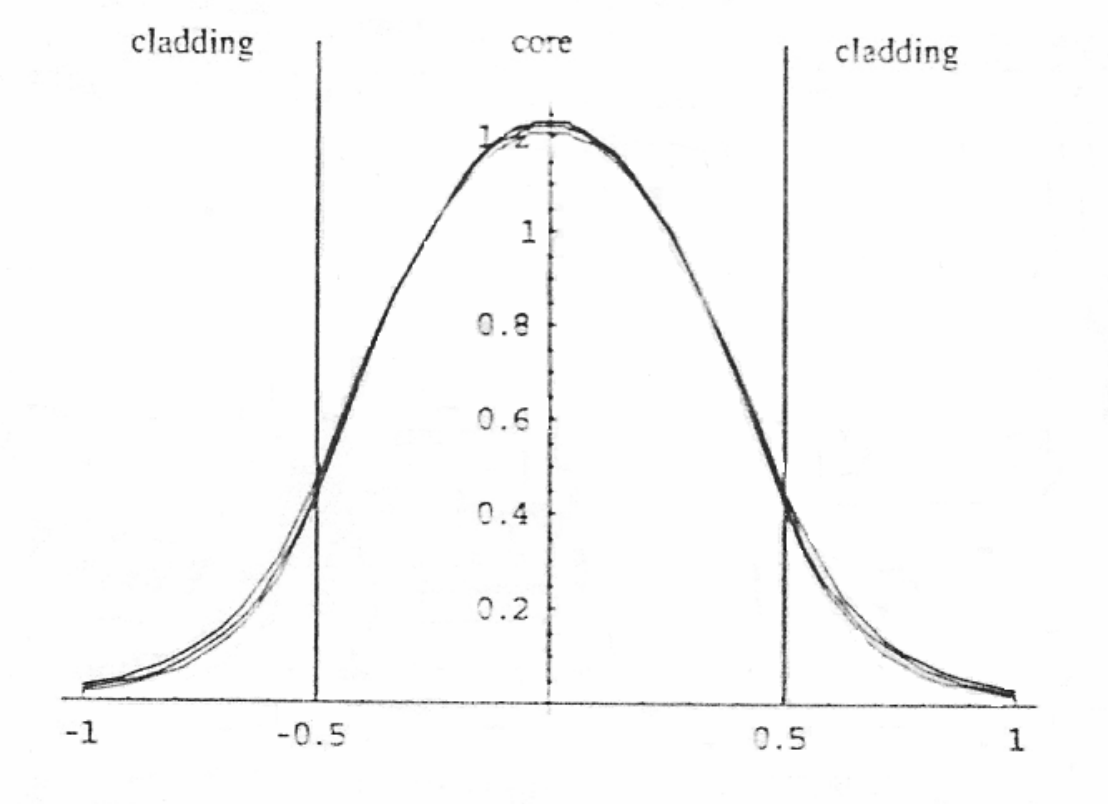

Fig.2.4: Normalized transverse field distributions of the fundamental modes (m = 0) for a symmetric planer optical waveguide under different hydrostatic stresses with t=1 μm . The curves from top are corresponding to $c_1\sigma = -0.01$, $c_1\sigma = 0$ and $c_1\sigma = 0.01$ stress values.

2.4 Evaluation of temperature sensitivity

Differentiating eqs. (2.8) with respect to the temperature, T, gives the temperature Sensitivity of the refractive index as [26]:

$$dn_{xx} / dT = Bn_0 - c_1 g_x E\Delta\alpha - c_2 (g_y + g_z) E\Delta\alpha, \tag{2.20.a}$$

$$dn_{yy} / dT = Bn_0 - c_1 g_y E\Delta\alpha - c_2 (g_x + g_z) E\Delta\alpha, \tag{2.20.b}$$

$$dn_{zz} / dT = Bn_0 - c_1 g_z E\Delta\alpha - c_2 (g_x + g_y) E\Delta\alpha, \tag{2.20.c}$$

Temperature Sensitivity is defined as the rate of change of the effective refractive index with respect to temperature. To evaluate Sensitivity we differentiae eqs. (2.16) with respect to the temperature ,T,

$$\frac{d}{dT}\left(\frac{p}{q}\right) = \frac{d}{dT}\left(\frac{1}{\tan\left(\frac{k_o t p}{2}\right)}\right),$$

and after some arrangement we find the relation as

$$\left[q + (p^2 + q^2) k_o t / 2\right] \frac{dp}{dT} = p \frac{dq}{dT} \tag{2.21}$$

this relation is applied for both even and odd modes. substituting for p, q, $\frac{dp}{dT}$ and $\frac{dq}{dT}$, and after some simplification we can find $\frac{dN}{dT}$ (which is temperature sensitivity (S_T)) expressed as:

$$S_T = A / B \tag{2.22}$$

Where, A = $(2\frac{dn_f}{dT}q^2 + \frac{dn_f}{dT}qp^2k_ot + \frac{dn_f}{dT}q^3k_ot + 2p^2\frac{dn_c}{dT})$ and

B= $(2q^2 + qp^2k_ot + q^3k_ot + 2p^2)$

As an example, we take $t = 1\mu m$, $\lambda = 0.83\,\mu m$, $dn_f / dT = 2\times10^{-5}1/^oc$,

$dn_c / dT = dn_s / dT = 1\times10^{-5}1/^oc$, $n_0 = 3.5$, and $n_c = 3$.

Then with a computer program we plot some relations like temperature sensitivity (S_T) as a function with a thickness of the core (t), also temperature sensitivity (S_T) as a function with effective refractive index (N) and effective refractive index (N)as a function with a thickness of the core (t) as shown in figures 2.5 and 2.6.

It is apparent from figures that the temperature sensitivity of the lower-order mode (m = 0) is higher than that of the higher – order mode (m = 2). Moreover, it is clear that from figure 2.5, sensitivity increases with the core thickness up to a limiting value when it become constant. From figure 2.6 there is a directly proportional between effective refractive index (N) and the core thickness of the waveguide. Also the same behavior between temperature sensitivity (S_T) and effective refractive index (N) appear in figure 2.7.

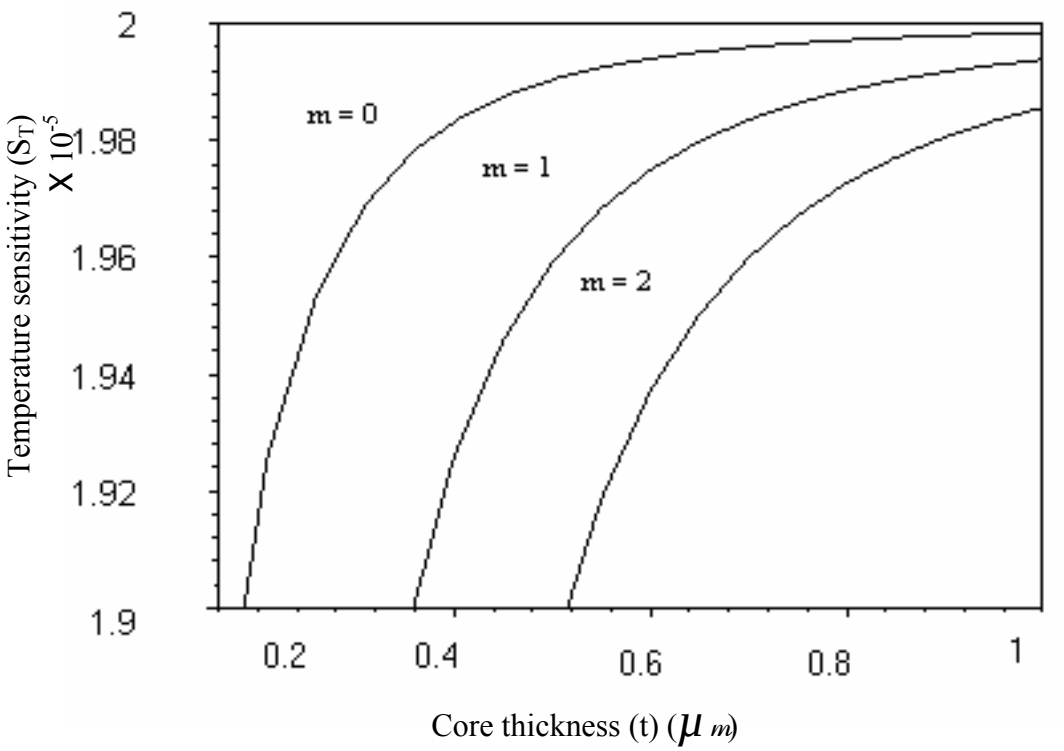

Fig.2.5: Temperature sensitivity (S_T) as a function of core thickness (t), for m=0,1,2.

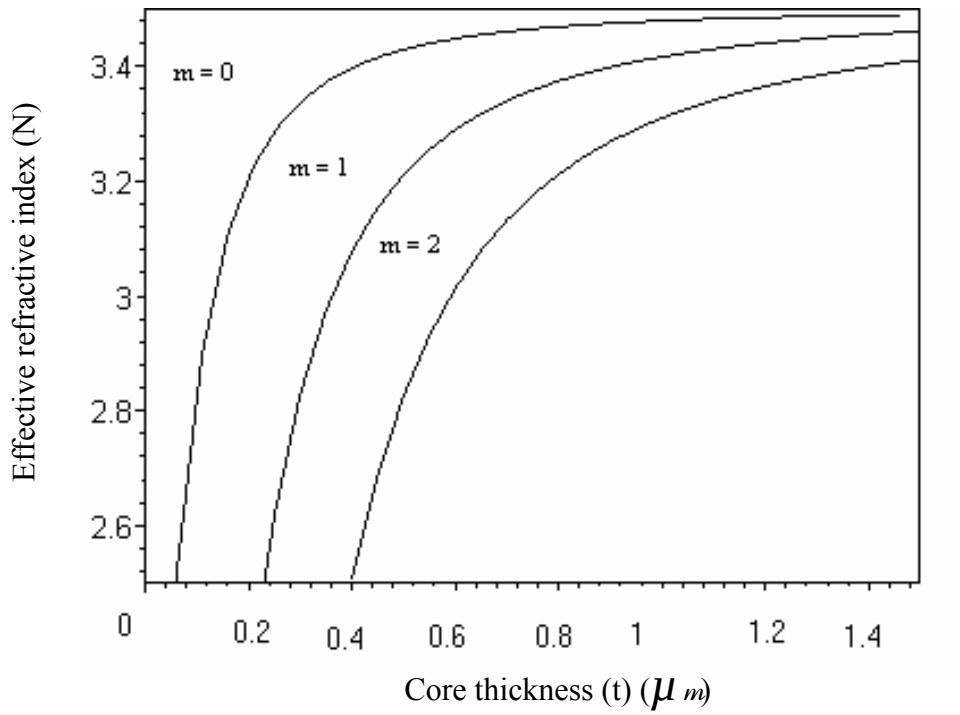

Fig.2.6: Effective refractive index (N) as a function of core thickness (t),for m=0,1,2.

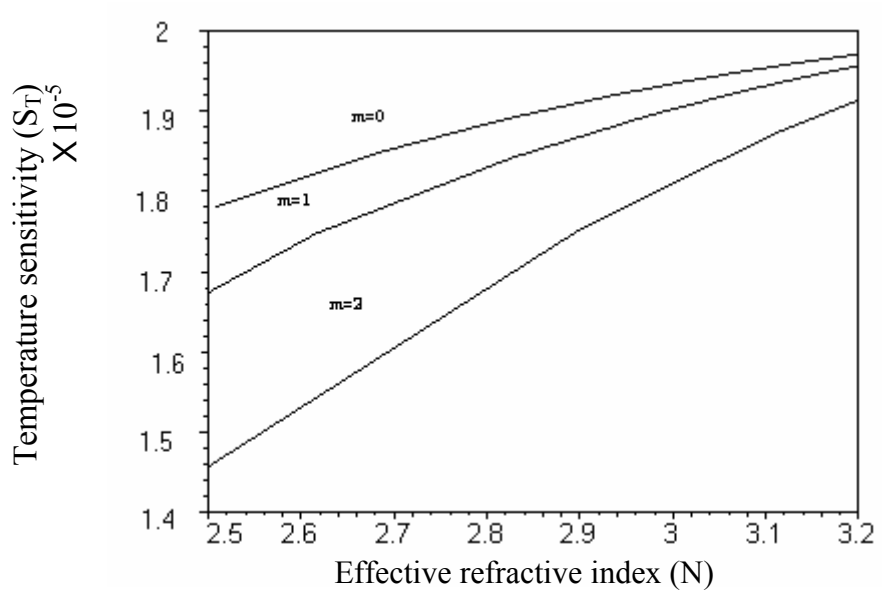

Fig.2.7: Temperature sensitivity (S_T)as a function of effective refractive index (N) for m = 0,1,2.

CHAPTER 3

Mathematical Simulation of Nonlinear Waveguide Sensors

In this chapter, an extensive theoretical and graphical analysis of nonlinear waveguide structure sensors is carried out. The waveguide sensor structure considered here without thermal stress effect and consists of a dielectric film bounded by a nonlinear cladding and a nonlinear substrate. The dispersion relation and sensitivity of nonlinear media are derived. The interface for nonlinear waves is also discussed. The power flow in nonlinear TE waves is calculated.

3.1 Dispersion equation of nonlinear planer waveguide

Suppose the structure of waveguide sensor is shown in figure 3.1 where a linear waveguide film is sandwiched between a nonlinear substrate and a nonlinear cladding with an intensity dependent refractive index whose dielectric function of the electric field is expressed as in eq. (1.12).

Consider the TE waves are propagate in the x-direction, with wave number k, and expressed as:

$$\mathbf{E} = (0, E_y, 0)\, exp[ik_0(N\,x\text{-}ct)], \tag{3.1}$$

In TE wave Maxwell's equations for cladding, core, and substrate respectively are given as [5, 15]:

$$\frac{\partial^2 E_y}{\partial z^2} - k_o^2\left(N^2 - \varepsilon_c\right)E_y + \alpha k_o^2\left(E_y^3\right) = 0 \qquad (z > t) \tag{3.2.a}$$

$$\frac{\partial^2 E_y}{\partial z^2} - k_o^2\left(N^2 - \varepsilon_f\right)E_y = 0 \qquad (0 \le z \le t) \tag{3.2.b}$$

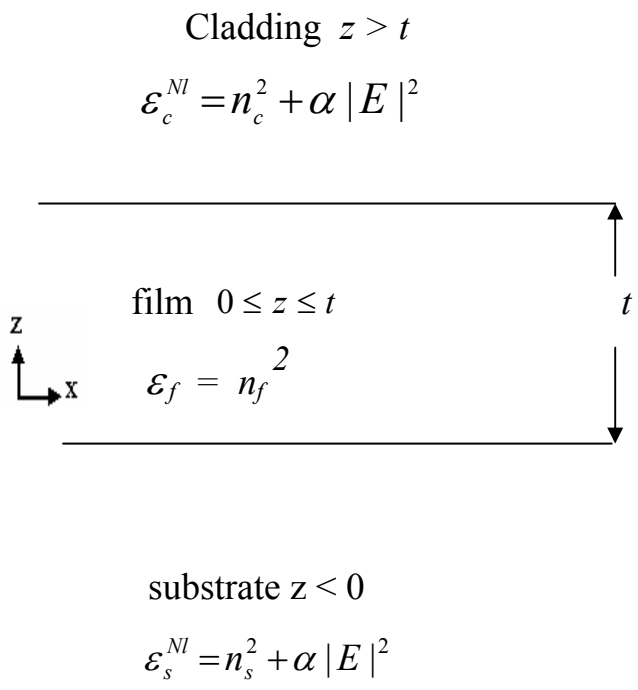

Fig.3.1: The waveguide structure under consideration.

$$\frac{\partial^2 E_y}{\partial z^2} - k_o^2 \left(N^2 - \varepsilon_s\right) E_y + \alpha k_o^2 \left(E_y^3\right) = 0 \qquad (z < 0) \qquad (3.2.c)$$

Solution of eq. (3.2.a) and eq. (3.2.c) is given [9, 31] by:

$$E_y = \sqrt{\frac{2}{\alpha_i}} \frac{q_i}{\cosh\left[k_o q_i (z - z_o)\right]} \qquad (3.3)$$

where z_o is a constant related to the power of the waveguide and $q_i = \sqrt{N^2 - \varepsilon_i}$, i = c, cladding and s, substrate.

If $N^2 > \varepsilon_f$, then the solution in the film medium is given by:

$$E_y = A_f \cosh(k_o pz) + B_f \sinh(k_o pz) \qquad (3.4)$$

where $p = \sqrt{N^2 - \varepsilon_f}$.

The continuity of both E_y and $\frac{\partial E_y}{\partial z}$ at the boundaries (z=0 and z=t) will give:

$$E_f = A_f \left[\cosh(k_0 pz) + \frac{q_s}{p} \tanh(k_0 q_s z_0) \cdot \sinh(k_0 pz)\right] \qquad (3.5)$$

Where $A_f = \sqrt{\frac{2}{\alpha}} \frac{q_s}{\cosh(k_0 q_s z_0)}$

$$E_c = \sqrt{\frac{2}{\alpha}} \frac{q_c}{\cosh\left[k_o q_c (z - z_o)\right]} \qquad (3.6)$$

$$E_s = \sqrt{\frac{2}{\alpha}} \frac{q_s}{\cosh\left[k_o q_s (z - z_o)\right]} \qquad (3.7)$$

From these equations, the dispersion equation is given as:

$$-\tanh(k_0 q_c (t - z_0)).q_c = \frac{\tanh(k_0 pt\ ) \cdot p + q_s \tanh(k_0 q_s z_0)}{1 + \frac{q_s}{p} \tanh(k_0 q_s z_0) \cdot \tanh(k_0 pt)} \qquad (3.\ 8)$$

To simplify this equation and to present the normalized formulae we will define [11, 17], two asymmetry parameters (a_s and a_c) and a normalized variable (X_s and X_c), are introduced as follows

$$X_c = \sqrt{\frac{N^2 - \varepsilon_c}{|\varepsilon_f - N^2|}} \quad , \quad X_s = \sqrt{\frac{N^2 - \varepsilon_s}{|\varepsilon_f - N^2|}} \qquad (3.9)$$

$$a_c = \frac{\varepsilon_c}{\varepsilon_f} \quad , \quad a_s = \frac{\varepsilon_s}{\varepsilon_f} \qquad (3.10)$$

a_c and a_s are defining normalized refractive index contrasts.

By use the relation between a normalized variable (X_s and X_c), and after some mathematics we reach to,

$$X_c = \sqrt{\frac{(1 - a_c)\left(1 + X_s^{\,2}\right)}{1 - a_s} - 1} \qquad (3.11)$$

$$X_s = \sqrt{\frac{(1 - a_s)\left(1 + X_c^{\,2}\right)}{1 - a_c} - 1} \qquad (3.12)$$

The effective refractive index N can be have the relation:

$$N = \sqrt{\frac{\varepsilon_g (a_c + X_c^2)}{1 + X_c^2}} \qquad (3.13\ )$$

By substituting about $q_i = \sqrt{N^2 - \varepsilon_i}$ and using eq. (3.11) and eq. (3.12), and after some mathematical arrangement the dispersion equation may be given by [5, 9, 16]:

$$k_o\, t \sqrt{\varepsilon_f} \sqrt{\frac{1-a_s}{1+X_s^{\,2}}} = \arctan(X_c \tanh(C)) + \arctan(X_s \tanh(C)) + m\pi \tag{3.14}$$

with $C = k_o (t - z_o)\sqrt{N^2 - \varepsilon_c}$ and m = 0,1,2,… . If the term (tanh(C)) in eq. (3.14) equal (±1) the problem will simplified to the linear dispersion equation.

3.2 The interface for nonlinear waves

For nonlinear waveguide we can study an important quantity it is the interface nonlinearity which can calculated from the electric field due to clad at the film-clad interface. We can replace with z = t in the field given from eq. (3.3). The result is [5, 9, 10]:

$$E_o = \sqrt{\frac{2}{\alpha}} \frac{q_c}{\cosh\left[k_o q_c (t - z_o)\right]} \tag{3.15}$$

by squaring both sides of eq. (3.15) and using the relation $[\cosh x]^{-2} = 1 - \tanh^2 x$, we can found that:

$$\frac{\alpha E_o^2}{2} = \frac{q_c^2}{\cosh^2[k_o q_c (t - z_o)]} = q_c^2 \{1 - \tanh^2[k_o q_c (t - z_o)]\} \tag{3.16}$$

From the dispersion equation eq. (3.14) one can substitute about tanh(C) in terms of $\frac{\alpha \ E_o^2}{2}$. Where from eq. (3.16) tanh(C) equal to [28- 32]:

$$\tanh(C) = \tanh(k_o q_c (t - z_o)) = \sqrt{1 - \frac{\alpha E^2}{2 q_c^2}} \tag{3.17}$$

Substituting for tanh(C) and making use of eq. (3.9) and eq. (3.10) we end with:

$$k_o t \sqrt{\frac{(1-a_s)\ \varepsilon_f}{1+\frac{N^2 - a_s \varepsilon_f}{|\ \varepsilon_f - N^2\ |}}} - \arctan\left(\sqrt{\frac{N^2 - a_s \varepsilon_f}{|\ \varepsilon_f - N^2\ |}} \sqrt{1 - \frac{\alpha\ E^2}{2\, q_c^2}}\right)$$

$$- \arctan\left(\sqrt{\frac{(1-a_c)\left[1+\left(\frac{N^2 - a_s \varepsilon_f}{|\ \varepsilon_f - N^2\ |}\right)\right]}{1-a_s}} - 1 \quad \sqrt{1 - \frac{\alpha\, E_o^2}{2(N^2 - a_c \varepsilon_f)}}\right) = 0 \tag{3.18}$$

This equation can be used to evaluate numerically N and conversely tanh(C) which will be used to give z_o.

3.3 The sensitivity for nonlinear waves

For homogeneous sensing, sensitivity (S_h) is evaluated as the rate of change of the effective refractive index of the waveguide (N) under an index change of the cover [18, 19], i.e.

$$S_h = \frac{\partial N}{\partial n_c} \tag{3.19}$$

Applying this to eq. (3.13) and after some arrangements, sensitivity can be expressed as [5]:

$$S_h(TE) = \frac{\sqrt{a_c}\,\sqrt{1+X_c^{\,2}}\,\tanh(C)}{X_c\,\sqrt{a_c+X_c^{\,2}}\,(1+X_c^{\,2}\tanh(C))\left(F_{TE}+\frac{1}{X_c}\frac{(1+X_c^{\,2})\tanh(C)}{(1+X_c^{\,2}\tanh(C))}+\frac{1}{X_s}\right)} \tag{3.20}$$

where F_{TE} = arctan $(X_c \tanh(C))$ + arctan $(X_s \tanh(C))$ + $m\pi$

3.4 Power flow of nonlinear TE waves

Researches showed a strong relationship between sensitivity and the power flow in the layers of the sensor is defined in ch.1 as:

$$P = \frac{1}{2}\int(\boldsymbol{E}\times\boldsymbol{H}^*)\;dz = \frac{1}{2}\int_{-\infty}^{\infty} E_y H_z^* dz$$

$$= P_s + P_f + P_c \tag{3.21}$$

H_z is given from Maxwell's equation (chapter 1) as:

$$H_z = \frac{k_o}{\mu_o\omega}\,E_y \tag{3.22}$$

By using E from eqs. (3.5), (3.6), (3.7), for $N^2 > \varepsilon_f$ and carrying out the integration one can result that [5, 33, 34]:

$$P_s = \frac{N\,q_c^2\,A^2}{2\mu_o\omega_o\,\alpha\,q_s\cosh^2(C)} \tag{3.23}$$

$$P_f = \frac{N q_c^2 A^2}{2\mu_o \omega_o \alpha \cosh^2(C)} \left[k_o h \left(1 - \frac{q_s^2}{q_f^2} \right) + \frac{\sinh(k_o q_f h)}{q_f} \left((1 + \frac{q_s^2}{q_f^2}) \cosh(k_o q_f h) + \frac{2 q_s}{q_f} \sinh(k_o q_f h) \right) \right] \tag{3.24}$$

$$P_c = \frac{N q_c}{\mu_o \omega \alpha} [1 - \tanh(C)] \tag{3.25}$$

$$, A_{TE} = F_{TE} + \frac{T \tanh(C)}{X_c} + \frac{1}{X_s} , \quad T = \frac{1 + X_c^2}{1 + X_c^2 \tanh(C)}$$

The fraction of the total power flowing through the cover region is related to the sensitivity.

CHAPTER 4

Effect of Thermal-Stress on Nonlinear Optical Waveguide Sensors

4.1 Introduction

The properties of waveguide sensing in dielectric films have been studied intensively for a number of years and have resulted in a large number of devices. To date, it has tacitly been assumed that the refractive indices associated with all of the media which constitute the waveguide sensors are independent of the local field intensity[6- 8]. Recently, dielectric film waveguides containing one or more media, whose refractive index depends on the local intensity, have stimulated a great deal of theoretical interest [17- 20].

Sensitivity for optical waveguide sensors has been obtained in many studies. Stress and thermal– stress effects on the sensitivity of linear optical waveguide sensors have been studied by Huang [8, 26].

In this chapter we study a planer structure of waveguide sensors containing a linear dielectric film that bounded by two nonlinear layers. We derive the dispersion relation for this structure and study the effect of stress on this structure and the effect of thermal– stress on temperature sensitivity.

4.2 The electric field in each layer of the medium

The dielectric function of a nonlinear media is characterized by eq .(1.11):

$$\varepsilon^{Nl} = \varepsilon^{L} + \alpha |E|^2$$

Figure 4.1 shows the configuration of the sensors under study. We assume a core of finite linear layer occupies the region $0 \le z \le t$. The

two surrounding nonlinear layers occupy the region z<0 and z>t as substrate and cladding respectively.

Only TE modes are going to be considered and these propagate along x- axis as:

$$\mathbf{E} = (0, E_y, 0)\, exp[ik_0(N x - cT)],$$

where $N = k/k_0$ is the effective index, k_o, c are the wave number and the speed of light in free space, respectively.

In TE waves, Maxwell's equations for cladding, core, and substrate respectively are given as [5, 15]:

$$\frac{\partial^2 E_y}{\partial z^2} - k_o^2\left(N^2 - \varepsilon_c\right)E_y + \alpha k_o^2\left(E_y^3\right) = 0 \qquad \text{(cladding)} \qquad (4.1)$$

$$\frac{\partial^2 E_y}{\partial z^2} - k_o^2\left(N^2 - \varepsilon_f\right)E_y = 0 \qquad \text{(core)} \qquad (4.2)$$

$$\frac{\partial^2 E_y}{\partial z^2} - k_o^2\left(N^2 - \varepsilon_s\right)E_y + \alpha k_o^2\left(E_y^3\right) = 0 \qquad \text{(substrate)} \qquad (4.3)$$

For $\alpha > 0$ the solution of eq. (4.1) and eq. (4.3) respectively is given as [9, 31]:

$$E_c = \sqrt{\frac{2}{\alpha}}\,\frac{q_c}{\cosh\left[k_o q_c (z - z_0)\right]} \qquad (4.4)$$

$$E_s = \sqrt{\frac{2}{\alpha}}\,\frac{q_s}{\cosh\left[k_o q_s (z - z_0)\right]} \qquad (4.5)$$

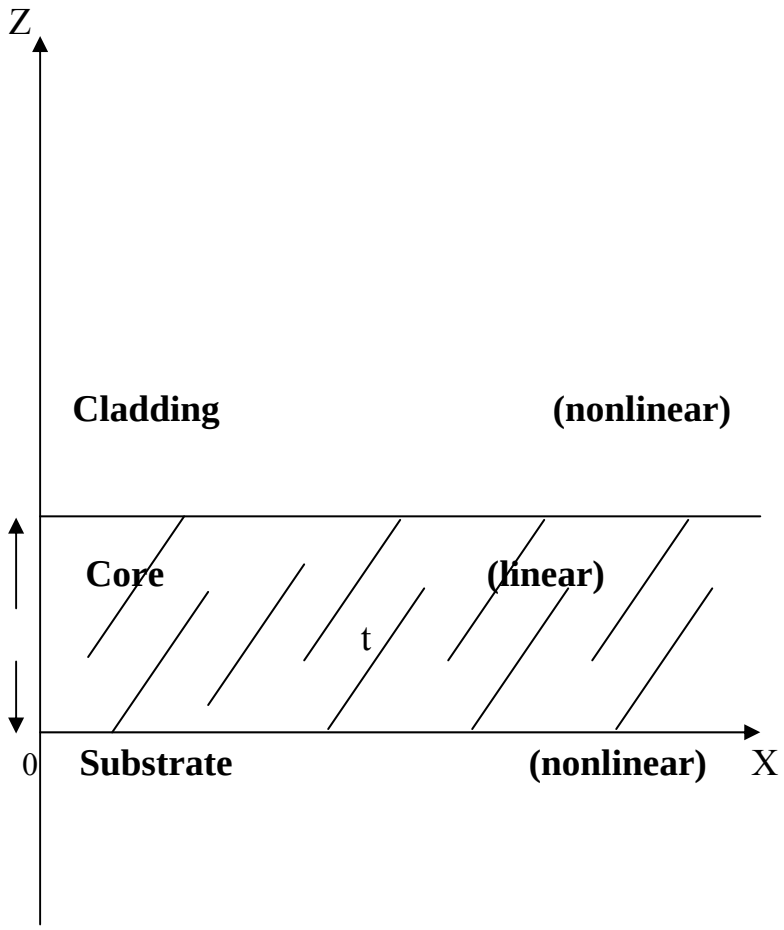

Fig.4.1 : Structure of the waveguide sensors, linear media bounded by two nonlinear cladding and substrate.

where $q_i = \sqrt{N^2 - \varepsilon_i}$, i=c, s which denotes to cladding and substrate respectively and z_0 is a constant related to the power of the waveguide (at $z = z_0$ the field is peak).

For $N^2 > \varepsilon_f$ the solution of eq. (4.2) is given as:

$$E_f = A_f \cosh(k_o p z) + B_f \sinh(k_o p z) \tag{4.6}$$

where $p = \sqrt{N^2 - \varepsilon_f}$ for the core.

Now to find the electric field in the core and the dispersion equation, there are four boundary conditions, to evaluate the constant A_f we relate this condition,

(1) $E_s(z = 0) = E_f(z = 0)$ and from eq. (4.4) and eq. (4.5),

$$\sqrt{\frac{2}{\alpha}} \frac{q_s}{\cosh[k_o q_s (z - z_0)]}(z=0) = A_f \cosh(k_o p z) + B_f \sinh(k_o p z)(z=0) \tag{4.7}$$

the result is:

$$A_f = \sqrt{\frac{2}{\alpha}} \frac{q_s}{\cosh(k_0 q_s z_0)} \tag{4.8}$$

To evaluate the constant B_f we relate the derivative of E_s and E_f,

(2) $\frac{\partial E_s}{\partial z}(z=0) = \frac{\partial E_f}{\partial z}(z = 0)$ where,

$$\frac{\partial E_s}{\partial z} = \sqrt{\frac{2}{\alpha}} q_s \frac{\partial}{\partial z}(\operatorname{sech}(k_0 q_s (z - z_0))) \tag{4.9}$$

but $\frac{\partial}{\partial x}(\operatorname{sech}(u) = -\operatorname{sech}(u)\tanh(u)\frac{du}{dx}$,

$$\frac{\partial E_s}{\partial z} = \sqrt{\frac{2}{\alpha}} q_s \cdot [-\text{sech}(k_0 q_s (z - z_0)) \cdot \tanh(k_0 q_s (z - z_0))] \cdot k_0 q_s \qquad (4.10)$$

$$\frac{\partial E_s}{\partial z} = \sqrt{\frac{2}{\alpha}} q_s \cdot [-\text{sech}(k_0 q_s (-z_0)) \cdot \tanh(k_0 q_s (-z_0))] \cdot k_0 q_s \qquad (4.11)$$

but sech(-u) = sech(u) , tanh(-u) = -tanh(u), where (u) for any function, then eq. (4.11) become:

$$\frac{\partial E_s}{\partial z} = \sqrt{\frac{2}{\alpha}} q_s \cdot [\text{sech}(k_0 q_s z_0) \cdot \tanh(k_0 q_s z_0)] \cdot k_0 q_s \qquad (4.12)$$

In a similar approach, we find:

$$\frac{\partial E_f}{\partial z} = A_f \sinh(k_0 p z) \cdot k_0 p + B_f \cosh(k_0 p z)] \cdot k_0 p \qquad (4.13)$$

$$\frac{\partial E_f}{\partial z}(z = 0) = B_f k_0 p \qquad (4.14)$$

Referring to the boundary condition $\frac{\partial E_s}{\partial z}(z = 0) = \frac{\partial E_f}{\partial z}(z = 0)$,

and from eq. (4.13) and eq. (4.15) then:

$$\sqrt{\frac{2}{\alpha}} q_s \cdot [\text{sech}(k_0 q_s z_0) \cdot \tanh(k_0 q_s z_0)] \cdot k_0 q_s = B_f k_0 p \qquad (4.15)$$

Which leads to:

$$B_f = \sqrt{\frac{2}{\alpha}} \frac{q_s}{p} \cdot [\text{sech}(k_0 q_s z_0) \cdot \tanh(k_0 q_s z_0)] \cdot q_s \qquad (4.16)$$

$$B_f = A_f \frac{q_s}{p} \tanh(k_0 q_s z_0) \qquad (4.17)$$

Finally, the electric field in the core film can be obtained from eq. (4.7), the result is,

$$E_f = A_f[\cosh(k_0 pz) + \frac{q_s}{p}\tanh(k_0 q_s z_0)\cdot\sinh(k_0 pz)] \qquad (4.18)$$

$$E_f = E_s(0)[\cosh(k_0 pz) + \frac{q_s}{p}\tanh(k_0 q_s z_0)\cdot\sinh(k_0 pz)] \qquad (4.19)$$

where E_s (0) is the electric field for substrate when z=0.

4.3 Dispersion relation

To relate the dispersion equation, we can use the third and fourth boundary conditions,

(3) E_c (z=t) = E_f (z=t)

(4) $$\frac{\partial Ec}{\partial z}(z=t) = \frac{\partial E_f}{\partial z}(z=t)$$

Substituting in the third condition, we get:

$$\sqrt{\frac{2}{\alpha}}\frac{q_c}{\cosh[k_o q_c(z-z_0)]} = \sqrt{\frac{2}{\alpha}}\frac{q_s}{\cosh(k_0 q_s z_0)}\ [\cosh(k_0 pz) + \frac{q_s}{p}\tanh(k_0 q_s z_0)\cdot\sinh(k_0 pz)] \qquad (4.20)$$

but $q_s = q_c$ then,

$$\frac{1}{\cosh[k_o q_c(t-z_0)]} = \frac{1}{\cosh(k_0 q_s z_0)}\cdot[\cosh(k_0 pt) + \frac{q_s}{p}\tanh(k_0 q_s z_0)\cdot\sinh(k_0 pt)] \qquad (4.21)$$

Also by substituting in the fourth condition, we get

$$\frac{\partial Ec}{\partial z}(z=t) = \frac{\partial E_f}{\partial z}(z=t),$$

$$\sqrt{\frac{2}{\alpha}}q_c \cdot [-\sec h(k_0 q_c (z-z_0) \cdot \tanh(k_0 q_c (z-z_0))] \cdot k_0 q_c =$$

$$\sqrt{\frac{2}{\alpha}} \frac{q_s}{\cosh(k_0 q_s z_0)} \cdot [\sinh(k_0 pz) \cdot k_0 p + \frac{q_s}{p} \tanh(k_0 pz_0) \cdot \cosh(k_0 pz) \cdot k_0 p] \tag{4.22}$$

$$-\sec h(k_0 q_c (t-z_0)) \cdot \tanh(k_0 q_c (t-z_0)) \cdot k_0 q_c =$$

$$\frac{1}{\cosh(k_0 q_s z_0)} \cdot [\sinh(k_0 pt) \cdot k_0 p + k_0 q_s \tanh(k_0 pz_0) \cdot \cosh(k_0 pt)] \tag{4.23}$$

Where:

$$\frac{\partial E_c}{\partial z} = \sqrt{\frac{2}{\alpha}} q_s \cdot [-\sec h(k_0 q_c (z-z_0) \cdot \tanh(k_0 q_c (z-z_0))] \cdot k_0 q_c$$

$$\frac{\partial E_f}{\partial z} = A_f \sinh(k_0 pz) \cdot k_0 p + B_f \cosh(k_0 pz)] \cdot k_0 p$$

Dividing eq. (4.23) by eq. (4.21), we result,

$$-\tanh(k_0 q_c (t-z_0)) \cdot k_0 q_c =$$

$$\frac{\sinh(k_0 pt) \cdot k_0 p + k_0 q_s \tanh(k_0 pz_0) \cdot \cosh(k_0 pt)}{\cosh(k_0 pt) + \frac{q_s}{p} \tanh(k_0 q_s z_0) \cdot \sinh(k_0 pt)} \tag{4.24}$$

Now, divining the right hand side of eq. (4.24) by $\cosh(k_0 pt)$, and after some arrangement, eq. (4.24) gives rise to:

$$-\tanh(k_0 q_c (t - z_0)) \cdot q_c = \frac{\tanh(k_0 pt\ ) \cdot p + q_s \tanh(k_0 p z_0)}{1 + \frac{q_s}{p} \tanh(k_0 q_s z_0) \cdot \tanh(k_0 pt)} \tag{4.25}$$

Equation 4.25 is called the dispersion equation of the system, and can take another form by taking (arctan) for both side of the last equation and after some arrangement we will rise to [5]:

$$k_0 tp - 2\arctan(\frac{q}{p}\tanh C) - m\pi = 0 \tag{4.26}$$

where $q = q_c = q_s$, m is the mode of the wave and take the value as 0, 1, 2,… .

4.4 Evaluation the temperature sensitivity for nonlinear medium

Temperature sensitivity is defined as the rate of change of the effective refractive index with respect to temperature. To evaluate the temperature sensitivity we differentiate the dispersion equation, eq. (4.26) with respect to temperature T, and making use the quantities p and q as a function of T that:

$p = \sqrt{N^2(T) - n_f{}^2(T)}$, $q = q_i = \sqrt{N^2(T) - n_1{}^2(T)}$,where $\varepsilon_f = n_f{}^2$ and $n_1{}^2 = \varepsilon_i$.

$$dp = (n_f . dn_f - N . dN) / p \tag{4.27}$$

$$dq = (N . dN - n_1 . dn1) / q \tag{4.28}$$

where dp is the differentiate of p with respect to T, dq is the differentiate of q with respect to T, dn_f is the differentiate of n_f with respect to T, dN is the differentiate of N with respect to T, and we can define it as the temperature sensitivity, S_T, and dn_1 is the differentiate of n_1 (refractive

index for cladding or substrate) with respect to T. Differentiate the dispersion equation, eq.(4.26) with respect to temperature T,

$$k_0 t dp - 2[\tanh(k_0 z_0 q) dq / p - q \tanh(k_0 z_0 q) dp / p^2 + (1 - \tanh(k_0 z_0 q) 2 q k_0 z_0 dq) / p] / [1 + (q^2 \tanh(k_0 z_0 q)^2 / p^2 \quad (4.29)$$

Substituting about dp and dq from eq. (4.28) and eq. (4.29), and dN = S_T and by means of a computer program to simplified it, finally we get the temperature sensitivity as,

$$ST = [F n_f dn_f q + G n_1 dn_1 p] / [N(Fq + Gp)] \quad (4.30)$$

Where, $$F = 1/2k_0 t(p^2 + q^2 \tanh(C^2)) + q \tanh(C) \quad (4.31)$$

$$G = \tanh(C) p + q(1 - \tanh(C^2) k_0 z_0 p \quad (4.32)$$

4.5 Stress effects on the performance of nonlinear waveguides

To study the stress magnitude effect on nonlinear waveguides we follow a similar approach as in section (2.3) and we assume that the core to be under hydrostatic stress state ,i.e., $\sigma_{xx} = \sigma_{yy} = \sigma_{zz} = \sigma$ and $\sigma_{xy} = 0$, the value of the refractive index in the core changes due to the $n_f = n_o - (c_1 + 2c_2)\sigma$. By substitute n_f in the quantity $p = \sqrt{N^2 - n_f^2}$ and consider the value of the stress can take two values ($c_1\sigma = -0.01$) and ($c_1\sigma = 0.01$), the ratio c_2 / c_1=0.1, finally we use the dispersion equation, eq. (4.26) and a computer program was used to plot the relation between effective refractive index (N) and a thickness of the core(t) for m =0, 1, 2.

CHAPTER 5

Results, Discussion and Conclusions

chapter two has described the dispersion relation for linear waveguide sensors and have evaluated the temperature sensitivity for such configuration. It also discussed the effect of stress on the core medium and then plotted some relations describing this case.

In chapter four, we derived the nonlinear characteristic dispersion equation eq. (4.25) and evaluated the value of temperature sensitivity eq. (4.29) , The effect of stress on the core region was also studied. These results are presented and studied numerically by means of a computer program maple V.

5.1 Numerical results for nonlinear temperature sensitivity

The mathematical study in the previous chapters is sufficient for describing and designing of the planer waveguide sensors. In computation, the data is used as reported by Huang [8, 26], where $n_1 = 2$, $\lambda = 0.83\mu m$, $dn_1 = 1 \times 10^{-5} 1/^o c$, $dn_f = 2 \times 10^{-5} 1/^o c$, $n_f = 3.5$. The core thickness (t) takes the values from 0 to 1.5 μm, also the quantity tanh(C) takes values between (-1 , 1) but we chose some of them, namely (0.3, 0.6, 0.55, 0.7, 0.9) and the dispersion relation eq. (4.25) can valid for any order of modes but we take m = 0, 1, 2 .

What we have actually done to plot temperature thermal sensitivity , we derived the dispersion eq. (4.25) with respect to temperature, then the derivative of the effective refractive index with respect to temperature called temperature sensitivity. A computer program was developed to plot temperature thermal sensitivity against various parameters. The appropriate equations are feed to the computers and we can get the results

plotted, we change parameters to study their effects. Moreover we carry out some graphs for comparison, we plotted the temperature sensitivity (S_T) as a relation between the quantities: core thickness (t) and effective refractive index (N) as shown in the following figures.

Figure 5.1.a shows how the temperature sensitivity varies with the core thickness (t), for order m = 0. From the figure the a directly proportional relation is apparent, that is; when the core thickness increases, the temperature sensitivity increases also. In the range of waveguide width less than 0.2 micrometer temperature sensitivity increases spontaneous with increasing width until the temperature sensitivity reach to maximum value after that, some sort of saturation takes place. This means that there is a considerable tolerance choosing the waveguide width which is get importance in manufacture. Figure 5.1.b also shows how the temperature sensitivity varies with the core thickness (t), for order m = 0, but for tanh (C) = 0.55, 0.7, 0.95. This figure tells us that there is a direct proportionality between temperature sensitivity and tanh (C) where when the value of tanh (C) is increased the peak of curve is increased too.

In figure 5.2, the relation between core thickness (t) and effective refractive index (N) is examined. The figure shows that relation for m = 0, 1, 2, and tanh (C) = 0.9. It's clear that when core thickness increases the effective refractive index increases also we found the largest peak is for m = 0.

Figure 5.3 shows another relation between core thickness (t) and effective refractive index (N) for m = 0 but we varied in the values of tanh (C), where (tanh (C) = 0.3, 0.6, 0.9) and found that there is a inverse relation, i.e when the value of tanh (C) is decreases the peak of curve increases.

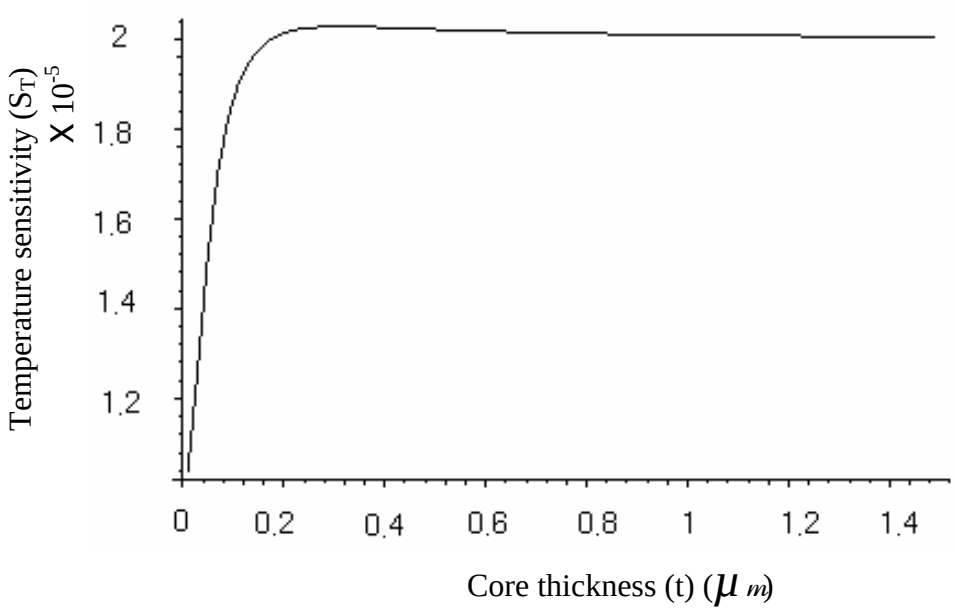

Fig.5.1.a: Temperature sensitivity (S_T)as a function of core thickness (t), for m=0 , and tanh (C) =0.9.

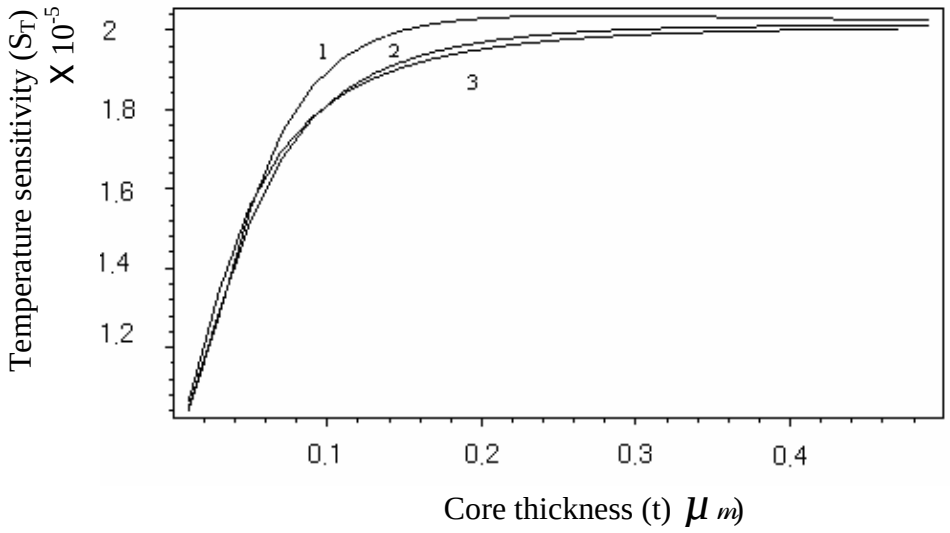

Fig.5.1.b: Temperature sensitivity (S_T)as a function of core thickness (t) for m=0 and for curve 1 tanh (C) = 0.95, for curve 2 tanh (C) = 0.7,and for curve 3 tanh (C) = 0.55

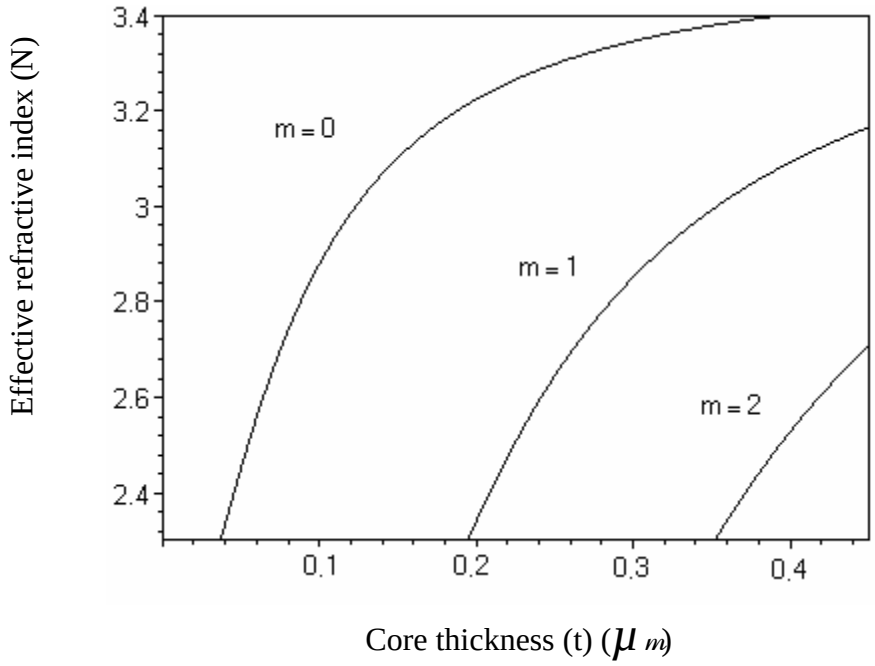

Fig.5.2: Effective refractive index (N) as a function of core thickness (t), for m=0,1,2,and tanh (C) = 0.9

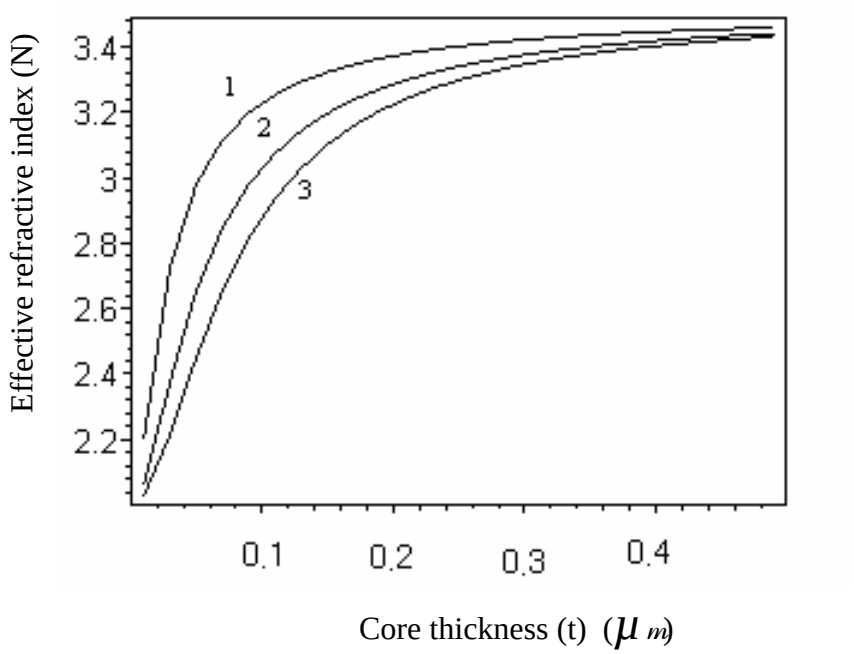

Fig.5.3: Effective refractive index (N) as a function of core thickness(t),for m=0, and tanh (C) = 0.3 (as in 1), tanh (C) = 0.6 (as in 2),and tanh (C) = 0.9 (as in 3).

After that we could plot a relation between temperature sensitivity (S_T) and the effective refractive index (N) as shown in figure 5.4, where m = 0, 1, 2 and tanh (C) = 0.7. it's clear that when effective refractive index (N) increases the temperature sensitivity (S_T) increases, also we found the largest peak is for m = 2.

Another relation between temperature sensitivity (S_T) and the effective refractive index (N) for m = 0 is shown in figure 5.5, in which we varied the values of tanh (C), where (tanh (C) = 0.3, 0.6, 0.9), there is a directly proportional between temperature sensitivity (S_T) and the effective refractive index (N) and found the largest peak for tanh (C) = 0.3.

Finally we made a comparison between linear and nonlinear media and described this difference by plotting some relations as shown in figure 5.6, figure 5.7 and figure 5.8.

Figure 5.6 shows a relation between temperature sensitivity and core thickness (t) for m = 0. From this figure we can see the described difference between linear and nonlinear media and we found that the peak of the nonlinear configuration is larger than linear one.

Also figure 5.7 shows a relation between temperature sensitivity and effective refractive index (N) for m = 0, the first curve for nonlinear media where tanh (C) = 0.9 and the second curve for the linear case. From the figure we found that the peak of the line for nonlinear sensors is larger than it is in the linear case.

In figures 5.6 and 5.7 we can explain the larger beak for the temperature sensitivity in the nonlinear curves for present the nonlinearity.

Another comparison between linear and nonlinear sensors is shown in figure 5.8, in which a relation between effective refractive index (N) and core thickness (t) for m = 0 was carried out. The curves 1, 2, 3 refer to the nonlinear configuration while curve 4 belongs to the linear case. We found that the linear case has the smallest peak that because the nonlinearity is present, where there is not that difference between it and the line of nonlinear (for tanh (C) = 0.9), so we can predict that the linear curve is the same as of nonlinear when tanh(C) =1, so from this figure we can reduced the describing difference between linear case and nonlinear, where the linear case and nonlinear can miserly when tanh(C) =1.

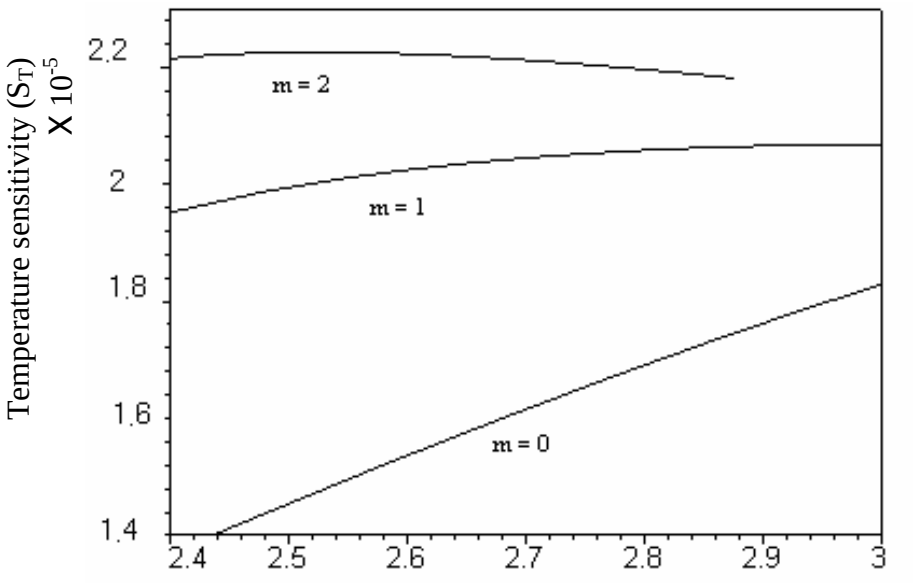

Fig.5.4: Temperature sensitivity (S_T)as a function of effective refractive index (N) for m=0,1,2, and tanh (C) = 0.7.

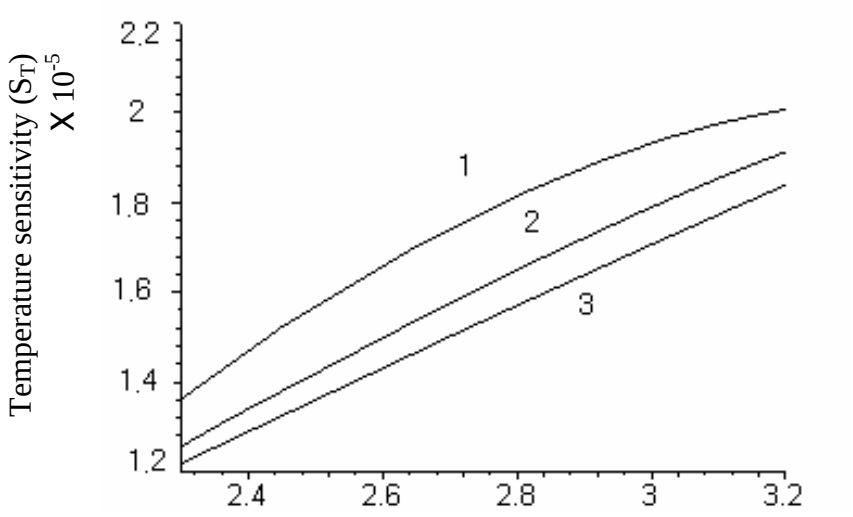

Fig.5.5: A relation between temperature sensitivity (S_T) and the effective refractive index (N) for m = 0 and for curve 1 tanh (C) = 0.3, for curve 2 tanh (C) = 0.6,and for curve 3 tanh (C) = 0.9.

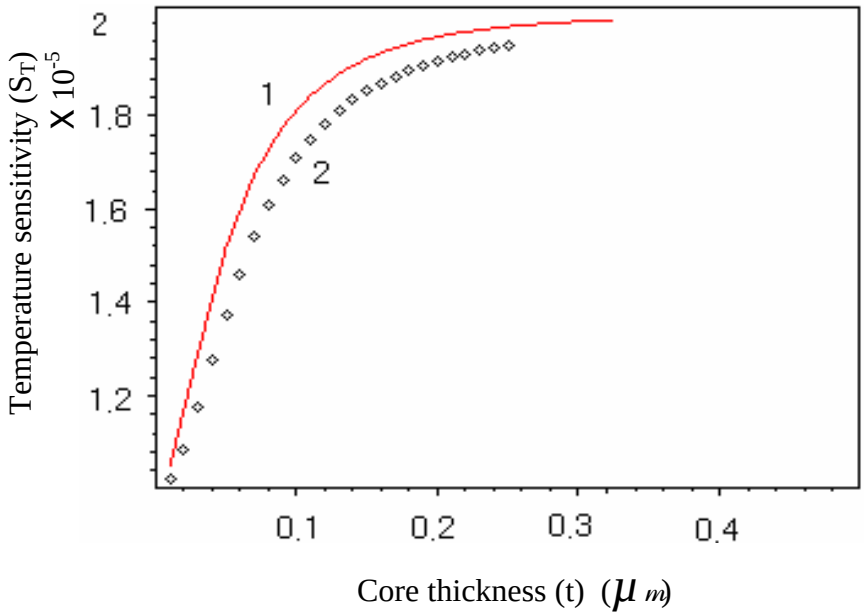

Fig.5.6: Temperature sensitivity (S_T)as a function of core thickness(t) for m=0,a solid line (curve 1) is for nonlinear sensor where, tanh (C) = 0.7and the squares (curve 2) is for linear sensor media (Huang).

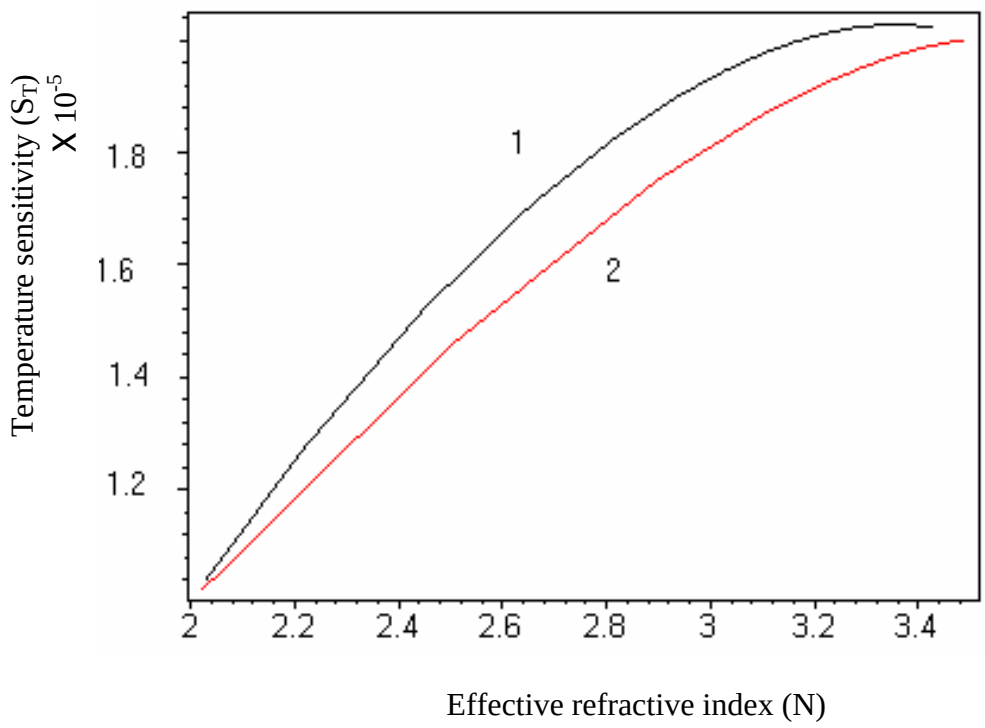

Fig.5.7: Temperature Sensitivity (S_T)as a function of the effective refractive index (N) for m = 0, curve 1 is for nonlinear sensor where, tanh (C) = 0.9 and curve 2 is for linear sensor.

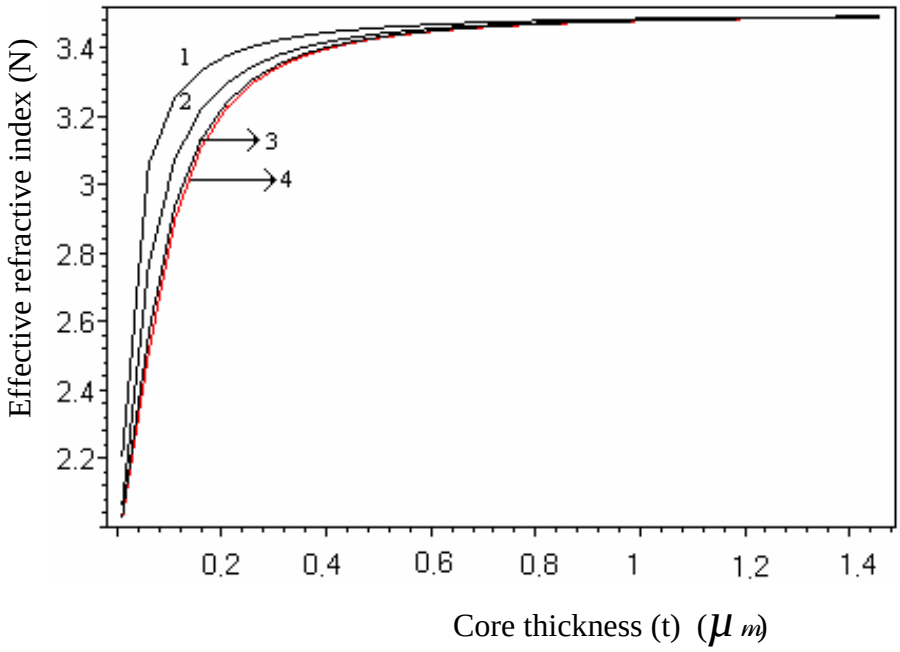

Fig.5.8: Effective refractive index (N) as a function of core thickness(t) for m=0,curves1,2,3 are for nonlinear sensor where for curve 1 tanh (C) = 0.3, for curve 2 tanh (C) = 0.6,and for curve 3 tanh (C) = 0.9 and curve 4 for linear sensor.

5.2 Numerical results for the Stress effects on nonlinear waveguides sensors

To describe the effect of stress on nonlinear waveguide sensors we assumed the core is under hydrostatic stress then the index of the core change due to stress i.e: $n_f = n_o - (c_1 + 2c_2)\sigma$, to plot it we revering to the desperation equation, eq. (4.26) and use the data as reported by Huang [8, 26], Where $n_1 = 2$, $\lambda = 0.83\,\mu m$, $n_0 = 3.5$, tanh(C) = 0.7, $n_f = n_o - (c_1 + 2c_2)\sigma$, $c_2/c_1 = 0.1$, the stress takes two values ($c_1\sigma = -0.01$) and ($c_1\sigma = 0.01$), and (t) takes the values from (0, 1.5 micro meter).

Figure 5.9 shows the effective refractive indexes as a function of core thickness for m = 0 , 1 , 2 and tanh (C) = 0.7, a comparison between different hydrostatic stresses take place, where the solid curves for positive stress while the dashed curves for negative stress. From the figure the mode wave m = 0 has a largest peak and the negative stress have peaks larger than the positive.

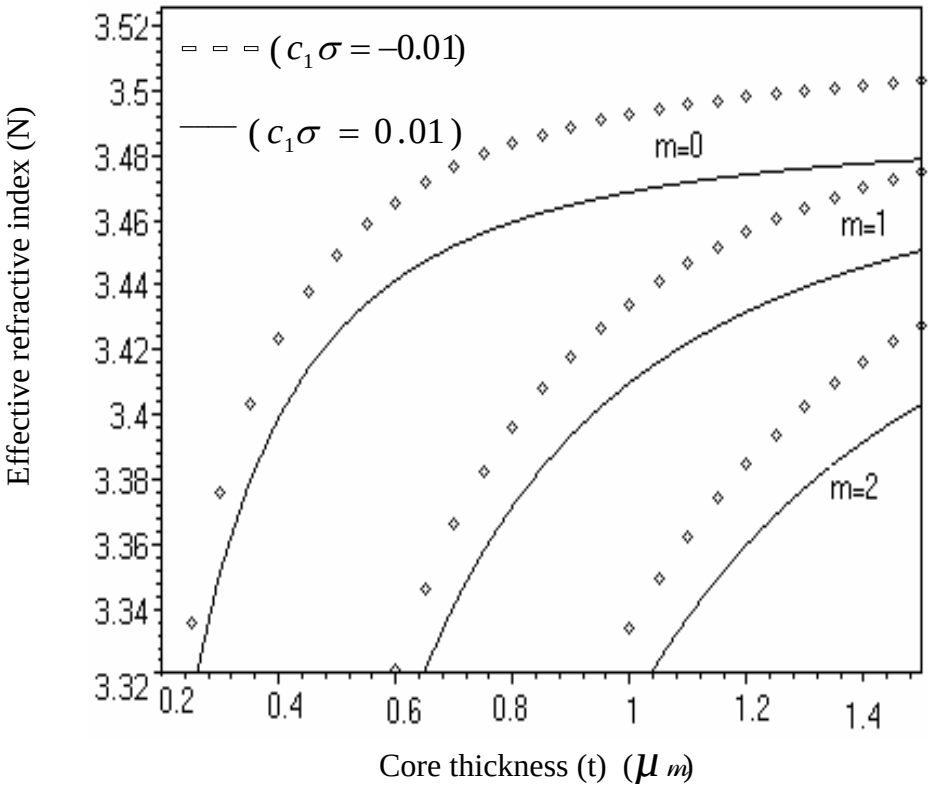

Fig.5.9: Effective refractive index (N) as a function of core thickness(t) for m=0,1,2, under different hydrostatic stresses.

5.3 Conclusion

The nonlinear optical waveguide sensors that the wave can propagate along the planer interfaces between different dielectric medium, in cases where at least one of the media is nonlinear, have attracted much attention. Plenty of papers have been devoted to deriving the dispersion equation and evaluating the sensitivity for various types of guided waves sensors in multi layered structure with nonlinear components.

Other papers investigated a new parameter to linear guided wave sensors, such as the effect of stress ,and thermal effect in which the temperature sensitivity was evaluated.

In this thesis, we have limited this work to TE waves. A mathematical and numerical analysis for propagation of electromagnetic wave along sensing structure which consists of a linear film bounded by two nonlinear cladding has been carried out. Dispersion equation has been derived theoretically. The propagation characteristics in the present three layers sensors were shown to be affected by stress and thermal – stress in which the effective refractive index exchanged and the temperature sensitivity evaluated.

We plotted temperature sensitivity with other parameter and found that there is a directly proportional between it and the quantities, as core thickness, effective refractive index. Also a directly proportional between effective refractive index and core thickness .

Comparison between linear and nonlinear sensors assumed and we can noticed that nonlinear sensors exhibit higher values of sensitivity,

these maxima, however, appear at smaller wave guiding widths this makes nonlinear sensors suitable for scientific and accurate sensing while linear configurations fit for commercial applications. Linear and nonlinear sensors do not differ at thick material(bulk), the values of effective refractive index in nonlinear sensors larger than it is in linear sensors. Finally depending on tolerance in choosing waveguide width, it is possible to manufacture cheap sensors with suitable sensitivity.

Future work :

One of the advantages of using planar optical waveguide sensors is that they are easily brought to maximum working point so there are some ideas that I suggest for future work like, the thermal stress effect may be shifted to multilayer planar waveguide sensors.

We can consider in future studying the other kinds of stress i.e.(in-plane, stress concentration, and pure shear) and Studying the effect of these kinds of stress on the sensitivity for nonlinear planer waveguide sensors. An interesting study may include evaluate the maximum sensitivity for our structure. In future we can applied the effect of thermal stress on surface sensors and a promising study may arise if coaxial fibers were considered.

REFERENCES

[1]- J. Love and A Shyder, Optical Waveguide theory, First edition, London: Chapman and Hall (1983).

[2]- J. D. Jackson, Classical Electrodynamics, Third edition, New York: John Wiley and Sons (1999).

[3]- J. R. Reitz, F. J. Milford, R. W. Christy, Foundations of Electromagnetic Theory, Third edition, New York: Wesley Publishing Company (1986).

[4]- C. Kittel, Introduction to Solid State Physics, Sixth edition, New Delh: Wiley Eastern Limited (1986).

[5]- M. M. Al-Abadla, Design of Nonlinear Guided Wave Sensors, (Ph. D. Desertion) (2004).

[6]- P. Martin and H. Bissessur, Appl. Phys **67**(**7**), pp.883 (1995).

[7]- O. Parriaux, and G. J. Veldhuis, J. of Light wave Tech **16**(**4**), pp.573-583 (1998).

[8]- M. Huang, International J. of Solids and Structures **40**, pp.1615 – 1632 (2003).

[9]- C. Seaton, J. D. valera, R. L. Shoemaker, G. I. Stegeman, J. T. Chilwell. And S. D. Smith, J. of Quantum Electronics **21**(**7**), pp.775 – 781 (1985).

[10]- G. I. Stegman, C. T. Seaton, W. H. Hetherington, A.D. Boardman, and P. Egan, J. Appl. Phys **27**, pp. 261 - 284.

[11]- F.Pigeon, Y. Jourlin and O. Parriaux, Thin Solid Films **394,** pp. 237 – 241 (2001).

[12]- R. Horvath, H. C. Pedersen, and N. Skivesen, Optics Letters **28**(**14**), pp.1233 – 1235 (2003).

[13]- R. Horvath and H. C. Pedersen, and N. Skivesen, App. Phy. Letters **81**(**12**), pp.2166 – 2168 (2002).

[14]- F. G. Bass, V. D. Freilikher. V. V. Prosentsov, Physics letters A **279**, pp.2453 – 2459 (1995).

[15]- G. I. Stegeman, C. T. Seaton, J. Ariyasu, R. F. Wallis and A. A. Maraduniu, J. Appl. Phys **58**(**7**), pp.2453 – 2459 (1985).

[16]- F. Lederer and D. Mihalache, Solid state communications **59**(**3**), pp. 151- 153 (1986).

[17]- M. M. Abadla, M. M. Shabat, and D. Jager, Microwave and Option Technology **5445**, pp. 324 – 327 (2003).

[18]- F. Prieto, A. Liobera, D. Jimenez, C. Domenguez, A. Calle, and L.M. Lechuga, J. of Light wave Technology **18**(**7**), pp. 966 – 972 (2000).
[19]- R. Horvath, L. R. Lindvold, and N. B. Larsen, Appl. Phys. B **74**, pp. 383 – 393 (2002).
[20] J. Ctyroky, J. Homola, M. Skalsky, Optical and Quantum Electronics **29**, pp. 301 – 311 (1997).
[21] - G. J. Veldhuis, O. Parriaux, H, J. W. M. Hoekstra. and P. V. Lambek, J. of Light wave Tech. **18**(**5**) (2000).
[22] - M. Allard, R. A. Masut, and M. Boudreau, J. of Light wave Tech **18**(**6**), pp. 813 – 818 (2000).
[23] - G. J.Veldhuis, O.Parriaux, P.V. Lambeck, Optical communications **163**, pp. 278 – 284 (1999).
[24] - F. Pigeon, I. F. Salakhutdinnv, and A.V. Tishchenko, J. of Applied Physics **90**(**2**), pp. 852 – 859 (2001).
[25] - S. K. Özdemir, and Gonul Turhan Sayan, J. of Light wave Technology **21**(**3**), pp. 805 – 814 (2003).
[26] - M. Huang, X. Yan, J. Opt. Soc. Am.B **20**(**6**), pp.1326 –1333 (2003).
[27] - G. I. Stegman and C. T. Seaton, J.Appl.Phys **58**(**12**), pp. 57 – 78 (1985).
[28] - O. N. Vassiliev and M. G. Cottam, Surface Review and Latters **7**(**1**), pp. 89 – 102 (2000).
[29] - A. D. Boardman, P. Egan, and R. F. Wallis, Applied Surface Science **65**(**66**), pp. 805 – 813 (1993).
[30] - W. Chen and A. A. Maradudiu, J. Opt. Soc. Am.B **5**(**2**), pp. 529 – 537 (1998).
[31] - A. D. Boardman, M. M. Shabat, and R. F. Wallis, Appl. Phys **24**, pp. 1702 – 1707 (1991).
[32] - D. Mihalache, R. G. Nazmidinov, and V. K. Fedyanin, Sov. J. Part. Nucl **20**(**1**), pp. 86 – 107 (1989).
[33] - S. Chelkowski and J. Chrostwski, Applied Optics **26**(**17**), pp. 3681 – 3688 (1987).
[34] - J. Ariyasu, C. T. Seaton and G. I. Stegman, J. Appl. Phys **58**(**7**), pp. 2463 – 2466 (1985).
[35] – H. j. El-Khozondar, R. J. El-Khozondar, M. M. shabat, and A. W. koch, Journal of Optical Communications, (in press).